PL-TR-93-2183
Environmental Research Papers, No. 1127

CONVECTION ALGORITHMS FOR MAGNETOSPHERIC PARTICLES

Kevin J. Kerns, Capt, USAF

10 August 1993

PHILLIPS LABORATORY
Directorate of Geophysics
AIR FORCE MATERIEL COMMAND
HANSCOM AIR FORCE BASE, MA 01731-3010

"This technical report has been reviewed and is approved for publication"

KEVIN J. KERNS, Capt, USAF
Contract Manager
Space Physics Division

E.G. MULLEN
Acting Director
Space Physics Division

This report has been reviewed by the ESC Public Affairs Office (PA) and is releasable to the National Technical Information Service (NTIS).

Qualified requestors may obtain additional copies from the Defense Technical Information Center. All others should apply to the National Technical Information Service.

If your address has changed, or if you wish to be removed from the mailing list, or if the addressee is no longer employed by your organization, please notify PL/TSI, 29 Randolph Road, Hanscom AFB, MA 01731 3010. This will assist us in maintaining a current mailing list.

Do not return copies of this report unless contractual obligations or notices on a specific document requires that it be returned.

REPORT DOCUMENTATION PAGE

Form Approved
OMB No. 0704-0188

1. AGENCY USE ONLY *(Leave blank)*	2. REPORT DATE	3. REPORT TYPE AND DATES COVERED
	10 August 1993	Scientific Interim

4. TITLE AND SUBTITLE
Convection Algorithms for Magnetospheric Particles

5. FUNDING NUMBERS
PE 62101F
PR 7601
TA 22
WU 03

6. AUTHOR(S)
Kevin J. Kerns, Capt, USAF

7. PERFORMING ORGANIZATION NAME(S) AND ADDRESS(ES)
Phillips Laboratory/GPSP
29 Randolph Road
Hanscom AFB, MA 01731-3010

8. PERFORMING ORGANIZATION REPORT NUMBER
PL-TR-93-2183
ERP, No. 1127

9. SPONSORING/MONITORING AGENCY NAME(S) AND ADDRESS(ES)

10. SPONSORING/MONITORING AGENCY REPORT NUMBER

11. SUPPLEMENTARY NOTES

12a. DISTRIBUTION/AVAILABILITY STATEMENT
Approved for public release; distribution unlimited

12b. DISTRIBUTION CODE

13. ABSTRACT *(Maximum 200 words)*

This report documents in detail the implementation of the convection model used for the research by Kerns, Hardy, and Gussenhoven titled "Modelling of Convection Boundaries Seen by CRRES in 120 eV to 28 keV Particles." This research is to be published in the Journal of Geophysical Research, Space Physics in 1993. The convection model assumes an Earth centered dipole magnetic field with equipotential field lines and a static cross tail electric field. Convection results from EXB drifts and magnetic field gradient and curvature drifts. Algorithms are provided to calculate drift paths of particles as well as to calculate the energy range of particles at a specified position that are on open drift paths to the magnetospheric tail. The algorithms presented in this document are optimized to converge to a solution quickly for any particle energy, position, and equatorial pitch angle. These algorithms are implemented in the CRRES survey software called SHOWLEPA.EXE which was used in support of the research.

14. SUBJECT TERMS
Plasma sheet, Magnetospheric convection, Electron, Proton

15. NUMBER OF PAGES
44

16. PRICE CODE

17. SECURITY CLASSIFICATION OF REPORT	18. SECURITY CLASSIFICATION OF THIS PAGE	19. SECURITY CLASSIFICATION OF ABSTRACT	20. LIMITATION OF ABSTRACT
UNCLASSIFIED	UNCLASSIFIED	UNCLASSIFIED	SAR

Contents

1. INTRODUCTION 1

2. CONVECTION MODEL 2

3. CALCULATION OF DRIFT PATHS 4

4. CALCULATION OF ELECTRON CUTOFF ENERGY, W_C . . 8

5. CALCULATION OF ION LOWER CUTOFF ENERGY, W_L . 18

6. CALCULATION OF ION UPPER CUTOFF ENERGY, W_H . . 24

7. CALCULATION OF ION STAGNATION ENERGY, W_S . . . 29

REFERENCES 35

Illustrations

1. Equipotentials for $A=7.46\text{x}10^{-5}$ V/m [Eq. (2)]. 6

2. Example of the iterative solution of Equation 9 for $Q=1.69$. 9

3. Convection paths of electrons measured at the white circle for six values of W_M. 11

4. ΔU as a function of L-shell at dusk ($\sin(\phi)=-1$) for the same conditions, measured location, and energies as those given for Figure 3. 12

5. Slope of Curve D in Figure 4. 15

6. Relationship between ΔU_P and W_M for the conditions given for Figure 4. 18

7. Convection paths of singly charged ions measured at the white circle for four values of W_M. 19

8. ΔU as a function of L-shell at dusk ($\sin(\phi)=-1$) for the same conditions, measured location, and energies as those given for Figure 7. 20

9. Slope of Curve B in Figure 8. 23

10. Relationship between ΔU_P and W_M for the conditions given for Figure 7. 25

11. Convection paths of singly charged ions measured at the white circle for six values of W_M. 26

12. ΔU as a function of L-shell at dawn ($\sin(\phi)=1$) for the same conditions, measured location, and energies as those given for Figure 11. 27

13. Slope of Curve E in Figure 12. The bold line is the actual slope, and the thin solid lines are approximations using Equation 15. 29

Figure 14 Relationship between ΔU_P and W_M for the conditions given for Figure 13. 31

Algorithms

1. Global constants and variables used by other algorithms, and names of parameters passed to functions and procedures given in other algorithms. 2

2. Implementation of I(y) given in Equation 4. 3

3. Implementation of Equations 3, 4, and 5. 5

4. Calculation of the L-shell of $\mathcal{L}_0$ for a local time specified by $\sin(\phi)$. 7

5. Calculation of the global variables L_0 and A. 8

6. Calculation of ΔU for given constants of motion and position. 10

7. Calculation of $\partial W/\partial L$ as a function of L-shell at dusk for a given set of constants of motion. 13

8. Calculation of L_P for given values of μ and J for electrons. . 14

9. Calculation of electron cutoff energy, W_C, for a position given by L, y, and $\sin(\phi)$. 17

10. Calculation of L_P at dusk for given values of μ and J for ions. 21

11. Calculation of ion lower cutoff energy ,W_L, for a position given by L, y, and $\sin(\phi)$. 24

12. Calculation of L_P at dawn for given values of μ and J for ions. 28

13. Calculation of ion upper cutoff energy, W_H, for a position given by L, y, and $\sin(\phi)$. 30

14. Calculation of ion stagnation energy, W_S, for a position given by L, y, and $\sin(\phi)$. 32

Acknowledgements

I would like to thank Lieutenant Jeralyn Meffert for all of her hard work in helping me to prepare this document.

Convection Algorithms for Magnetospheric Particles

1. INTRODUCTION

This report documents in detail the implementation of the convection model used in the research conducted by Kerns, Hardy, and Gussenhoven [1993]. The convection model assumes an Earth-centered dipole magnetic field with equipotential field lines, and it assumes a static cross tail electric field of the form $V \propto L^{\gamma}\sin(\phi)$ where γ is a positive real number, L is L-shell (see McIlwain [1961]), and ϕ is local time. Convection occurs because of $\mathbf{E}\times\mathbf{B}$ drifts and magnetic field gradient and curvature drifts. The model is used to calculate drift paths of particles as well as to calculate the range of kinetic energy for which ions and electrons move on drift paths open to the magnetospheric tail. Drift paths are calculated using conservation of the first two adiabatic invariants [Chen, 1984] and conservation of energy. Electrons are shown to be on open drift paths if the kinetic energy, W, is $0 < W < W_C$ where W_C is the electron cutoff energy, and ions are on open drift paths if $W_L < W < W_H$ where W_L and W_H are the ion lower and upper cutoff energies respectively. The algorithms presented in this document are optimized to converge to a solution quickly for any positive real value of γ, for any particle energy, position, and equatorial pitch angle, and for any cross-tail field strength. These algorithms are used by the CRRES survey software called "SHOWLEPA.EXE" which was developed by this author at the Phillips Laboratory in support of the research by Kerns, Hardy, and Gussenhoven [1993].

Implementations of equations are given in algorithms that are listed in text boxes separate from the main text. These algorithms are written in pseudo-code similar to Pascal to make them readable to the non-programmer and useable to the programmer; comments are given in italics and are not considered part of the instructions or code. These are added to make the code more readable. Constants are defined at the top of any procedure or function using the "$\equiv$" symbol, and each constant represents a value that does not change. Constants are used to reduce unnecessary math to make the code execute more quickly. All variables are assumed to contain real values unless specifically identified as integers, and the variables required for any given function or procedure are listed near the top of the code for that procedure or function. Algorithms use logical, not

Received for publication 3 August 1993

mathematical, statements so that the statement "i=i+1", which is nonsense in mathematics, means to increment the value contained in the variable called "i" by 1. Subscripts are part of variable names, and are used to make code more readable. The one exception to the use of subscripts is with the table of values for the function I(y) given in Algorithm 1; here subscripts are used to identify individual elements of the table. Function and procedure names are given in bold letters, and all parameters passed to these use the naming convention given in Algorithm 1. The ***repeat block until condition*** loop implements a block of code once, and then continues to re-implement the same block until the given condition is true. The ***while condition block*** iterates the next block of code for as long as the given condition is true. The ***if condition then code*** statement implements the block of code only if the condition is true, and the ***if condition then code1 else code2*** statement implements the "code1" block of code if the condition is true and the "code2" block of code otherwise. All blocks of code that are longer than one line, with the exception of those bounded by "**repeat . . . until**" loops, are marked by "**begin**" and "**end**" statements . Indentation is used to make loops and blocks more readable. Nested parentheses are made more readable by using "{ [(..)] }".

2. CONVECTION MODEL

In this section the model used to calculate the trajectories of central plasma sheet

Algorithm 1 Global constants and variables used by other algorithms, and names of parameters passed to functions and procedures given in other algorithms.

Global constants used in all calculations and algorithms:

$\omega \equiv 7.272X10^{-5}$	*radians per second, Earth's spin rate*
$a \equiv 6.378X10^{6}$	*meters, Earth's radius*
$B_0 \equiv 3.1X10^{-5}$	*tesla, magnetic field at Earth's Equator*
$I_i \equiv I(i/N);\ 0 \le i \le N$	*I() defined in Algorithm 2; "i" is element index of table.*
$N \equiv 1000$	*I_0 is first element, and I_N is last element of table.*
$\delta_L \equiv 0.01$	*R_E, error allowed in calculating L-Shells*
$\delta_W \equiv 0.001$	*eV, error allowed in calculating cutoff energies*
$W_{step} \equiv 10000$	*eV, energy step used in cutoff solutions*

Global variables used in all calculations and algorithms:

A	*volts/meter, from Equation 2*
γ	*from Equation 2*
L_0	*from Equation 7*

Standardized names of parameters passed to functions and procedures:

y	*sine of equatorial pitch angle, (0.0 ≤ y ≤ 1.0), (Equations 3 and 4)*
s	*sine of local time; sin(π/12·LT), (-1.0 ≤ s ≤ 1.0)*
W	*kinetic energy in eV*
L	*L-shell in R_E*
μ	*first adiabatic invariant constant (Equation 3)*
J	*second adiabatic invariant constant (Equation 4)*
U	*total energy of particle in eV (Equation 5)*
electron	*boolean; true if particle is an electron and false if it is an ion.*

(CPS) particles in the inner magnetosphere under conditions of steady convection is described. The model follows the same method and assumptions used by Volland [1973]. It assumes a dipole geomagnetic field aligned with the Earth's spin axis and having equipotential field lines. The co-rotation electric field potential is then taken as

$$V_\omega = B_o a^2 \omega L^{-1}, \tag{1}$$

where B_0 is the strength of the equatorial magnetic field at the surface of the Earth, a is the Earth's radius, ω is the Earth's spin rate, and L is L-shell in R_E. The cross-tail potential is assumed to be of the form given by Volland [1973]

$$V_\gamma = aAL^\gamma \sin(\phi) \tag{2}$$

where A scales the field strength, γ determines the rate of decrease in potential with decreasing altitudes, and ϕ is the local time. The model is used to determine the range of kinetic energy of ions and electrons in which the particles convect on open drift paths from the tail. The bounds of this range are referred to as cutoff energies, and these are a function of the position at which the particle is measured as well as the parameters A and γ of Eq. (2). Cutoff energies for steady convection have been introduced previously in other works including Stern [1975] and Southwood and Kaye [1979]. In all examples given in this report, $\gamma=2$, after Stern [1975], and the values of the constants in Eqs. (1) and (2) are given in Algorithm 1. The values of A and γ are given as global variables in Algorithm 1, and these are used by the subsequent algorithms. These values are scaled to represent different magnetospheric conditions. In addition to the values of the constants used, Algorithm 1 contains the standard names of parameters passed to the functions given in subsequent algorithms.

Algorithm 2 Implementation of I(y) given in Equation 4.

```
FUNCTION DEFINITION OF I(y)
local constants required for I(y):
        α ≡ 1.380173                    ß ≡ ½α - 0.3702402
        a1 ≡ 0.055   a2 ≡ -0.037   a3 ≡ -0.074   a4 ≡ 0.056
        b0 ≡ 2α      b1 ≡ 3a1      b2 ≡ 6a2      b3 ≡ 4ß-2α-3a1-6a2+6a4
        b4 ≡ -6a4    bL ≡ 2(ß-a3)  b½ ≡ -4ß
local variables required for I(y):
        yL, yC, I
implementation of I(y):
        if y = 0.0 then
                I = b0
        else if y = 1.0 then
                I = 0.0
        else
                begin conditional block
                yL = ln(y)                  ln(x) is natural logarithm of x
                yC = exp(⅓yL)               exp(x) is inverse natural logarithm or e^x
                I = b0 + {b1 + [b2 + (b3 + bL·yL + b4·yC)·yC]·yC}·yC + b½·y^½
                end conditional block
        return value of I
```

Particle motion is assumed to be a combination of $\mathbf{E}\times\mathbf{B}$ drift and magnetic field gradient and curvature drift. Trajectories are determined by conservation of energy and conservation of the first two adiabatic invariants. From these the three following constants of motion are defined:

$$\mu = y^2 W L^3 \tag{3}$$

$$J = W^{1/2} L I(y) \tag{4}$$

$$U = W + q[aAL^{\gamma}\sin(\phi) - L^{-1}B_0 a^2\omega] \tag{5}$$

where μ and J are proportional to the first two adiabatic invariants, U is the total energy, y is the sine of the equatorial pitch angle, W is kinetic energy, and q is charge. Ions are assumed to be singly ionized so that $q=\pm 1$ for ions and electrons respectively. The function I(y) in Eq. (4) is an integration function of the bounce motion, and the approximation given by Ejiri [1978] is used for the implementation shown in Algorithm 2. Equation (5) is the sum of the kinetic energy and potential energy [Eq. (1) and (2)].

3. CALCULATION OF DRIFT PATHS

Valid drift paths of particles are the set of all points where Eqs. (3), (4), and (5) give $\mu=\mu_M$, $J=J_M$, and $U=U_M$. These constants of motion are for a particle with measured kinetic energy $W=W_M$ at a position $L=L_M$, $\sin(\phi)=\sin(\phi_M)$, and $y=y_M$. Algorithm 3 shows the implementation of these equations. Here the function I(y) from Eq. (4) is replaced by a look-up table with N+1 equally spaced elements, and the value of I(y) is found by interpolating between the two nearest table elements. This table is used to make the algorithms faster.

The simplest case of convection is for zero kinetic energy particles ($W_M=0$), and this is presented first. From Eqs. (3) and (4), $\mu_M=J_M=0$, and conservation of energy [Eq. (5)] requires that these particles drift on equipotential lines given by

$$V = aAL^{\gamma}\sin(\phi) - L^{-1}B_0 a^2\omega \tag{6}$$

Figure 1 shows the equipotentials given by this equation for $A=7.46\times10^{5}$ V/m. In this figure, noon is towards the top of the page and each hour of LT is marked by a radial line. The half shaded circle represents the Earth, and the concentric circles show L-shells 2 through 9 R_E. The heavy lines show equipotentials from -45 kV to 5 kV at 5 kV intervals, and these are symmetric about the dawn-dusk line. In this example, the three lines shown closest to the Earth (-45 to -35 kV) are closed, and zero kinetic energy particles on these lines are trapped and drift around the Earth in an Eastward direction. The equipotential lines further from the Earth are open, and zero kinetic energy particles on these are not trapped, but drift sunward from the tail until they encounter the magnetopause.

Algorithm 3 Implementation of Equations 3, 4, and 5.

```
FUNCTION DEFINITION OF μ(γ, W, L)                    Equation 3.
implementation of μ(γ, W, L):
        return value of (γ·L)²·L·W

FUNCTION DEFINITION OF J(γ, W, L)                    Equation 4.
local variables required for J(γ, W, L):
        I_r     value of I(γ) interpolated from the array I_i (Algorithm 1)
        i       index of element in I_i to be used for interpolating I_r
implementation of J(γ, W, L):
        if γ = 0.0 then
                I_r = I_0
        else if γ = 1.0 then
                I_r = I_N
        else
                begin conditional block
                I_r = N·γ               N is maximum index of I (Algorithm 1)
                i = trunc(I_r)          trunc returns the largest integer less than
                I_r = I_r - i                   or equal to I_r
                I_r = I_i·(1-I_r) + I_i+1·I_r   I_r now contains interpolated value of I(γ)
                end conditional block
        return value of W^½·L·I_r

FUNCTION DEFINITION OF U(electron, W, L, s)          Equation 5.
local variables required for U(electron, W, L, s):
        k ≡ B_0·a²·ω
implementation of U(electron, W, L, s):
        if electron then                                    see Algorithm 1
                return value of W - a·A·s·L^γ + k/L         q = -1
        else
                return value of W + a·A·s·L^γ - k/L         q = +1
```

The zero energy Alfvén layer, $\mathcal{L}_0$, is the last closed drift path for zero kinetic energy particles. In Figure 1, $\mathcal{L}_0$ is tear-drop shaped and lies along the -30 kV equipotential, and it bounds the shaded region that surrounds the Earth. $\mathcal{L}_0$ at dusk (1800) is a stagnation point for W=0 particles because here the corotation electric field is equal and opposite to the cross-tail field resulting in no electric field drift; Ejiri [1978] derives the L-shell of this point, L_0, as:

$$L_0 = \left[\frac{\omega a B_o}{\gamma A}\right]^{\frac{1}{\gamma+1}} \tag{7}$$

The value of L_0 is used, instead of the value of A, to indicate the cross-tail field strength in the remaining examples because A can be determined from Eq. (7), and its value scales with the distance of $\mathcal{L}_0$ from the Earth. L_0=4.58 R_E in Figure 1.

The L-shell of $\mathcal{L}_0$ can be determined for any local time by using Eqs. (6) and (7). The potential, $V_{\mathcal{L}}$, of $\mathcal{L}_0$ is found by substituting L_0 for L, and -1 for $\sin(\phi)$ in Eq. (6). As is evident in Figure 1, $\mathcal{L}_0$ is at maximum L-shell at dusk, so that L_0 is always greater than or equal to the L-shell of $\mathcal{L}_0$ for the given local time. Solving for the partial of V

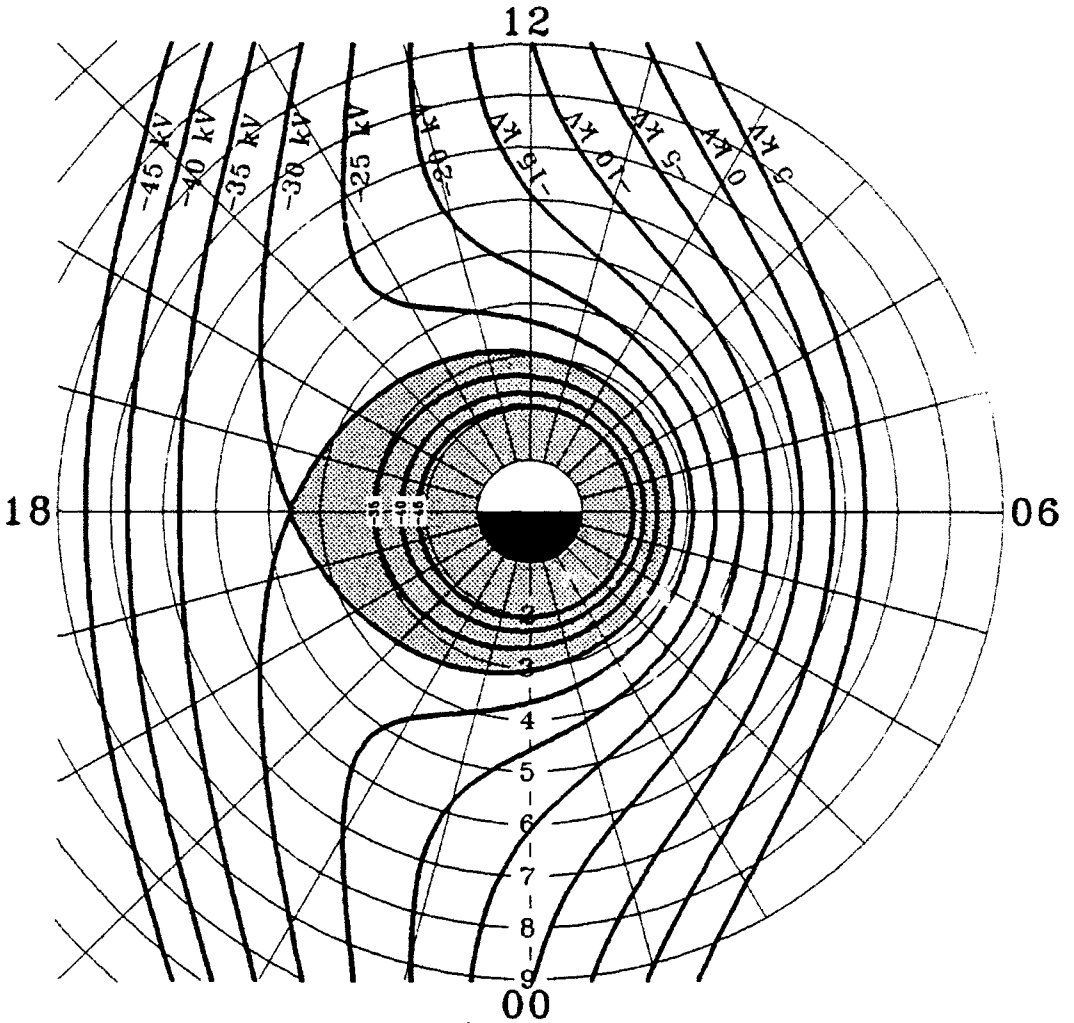

Figure 1 Equipotentials for $A=7.46\text{x}10^{-5}$ V/m [Eq. (2)]. Radial distance shows L-shell in R_E, and angular distance shows local time. The shaded region is bounded by $\mathcal{L}_0$.

[Eq. (6)] with respect to L and setting the result equal to zero gives

$$L_{\partial V/\partial L=0} = \left[\frac{\omega a B_0}{-\gamma A \sin(\phi)} \right]^{\frac{1}{\gamma+1}} \tag{8}$$

This equation shows that the slope of V as a function of L in Eq. (7) does not change sign on the dawn side ($\sin(\phi) \geq 0$) because $\partial V/\partial L$ cannot equal zero. On the dusk side ($\sin(\phi) < 0$), Eq. (8) shows that the L-shell at which the slope changes sign ($\partial V/\partial L=0$) must be greater than L_0 [Eq. (7)]. Because the slope does not change sign in the region where the valid solution exists ($0 \leq L \leq L_0$), a simple binary search can be used to determine the L-shell at a given local time with the same potential as that for L_0 at dusk. The starting limits of L-shell for the search are 0 and L_0, and the implementation is shown in Algorithm 4. This algorithm assumes that the values of A, γ, and L_0 have been

Algorithm 4 Calculation of the L-shell of $\mathcal{L}_0$ for a local time specified by sin(ϕ).

```
FUNCTION DEFINITION OF L_ℒ(s)
local constants required for L_ℒ(s):
        k = -B_0·a^2·ω
local variables required for L_ℒ(s):
        k_s, V, V_ℒ, ΔL_ℒ, L_ℒ
implementation of L_ℒ(s):
        V_ℒ = k/L_0 - a·A·L_0^γ      potential of ℒ_0 is found from Equation 6
        k_s = a·A·s                  These multiplications are done before the loop
        L_ℒ = L_0                    highest possible value for L_ℒ
        ΔL_ℒ = L_0                   step size assuming lowest possible value of L_ℒ is zero.
        if s>-0.999999 then          Prevent round off error from causing a run-away loop.
                repeat the following loop:
                        V = k/L_ℒ + k_s·L_ℒ^γ     potential from Equation 6 at sin(φ) = s
                        ΔL_ℒ = ½·ΔL_ℒ            the step size halves during each iteration
                        if (V > V_ℒ) then
                                L_ℒ = L_ℒ - ΔL_ℒ        L_ℒ should be smaller
                        else
                                L_ℒ = L_ℒ + ΔL_ℒ        L_ℒ should be larger
                until ΔL_ℒ < δ_L        The loop is terminated once sufficient accuracy
        return value of L_ℒ             is reached, and the value of L_ℒ is returned.
```

previously determined. A similar algorithm not shown in this report was used to plot the equipotential lines in Figure 1. Algorithm 5 shows the implementation of Eq. (7) to set the value of the global variable L_0, when A and γ are known. It also shows a simple method of determining the values of L_0 and A when only γ is known so that $\mathcal{L}_0$ includes a specified L-shell and local time. It uses a binary search to determine the value of A that results in a value of $L_{\mathcal{L}}(s)$ (Algorithm 4) equal to L.

When $W>0$, Eqs. (3), (4), and (5) must be solved simultaneously to determine the drift paths of a particle measured with the constants of motion, μ_M, J_M, and U_M. Equations (3) and (4) are first combined to solve for y as a function of L-shell.

$$I(y)y^{-1} = J_M\mu_M^{-½}L^{½} = Q \tag{9}$$

Equation (9) can be solved analytically if the function I(y) is assumed to be linear such that $I(y) \approx a_l + b_l y$. The solution of y is then

$$y \approx a_l(Q-b_l)^{-1} \tag{10}$$

The values of a_l and b_l are determined using the two elements of table I (Algorithm 1) nearest to the solution of y. This method leads to an iterative solution which is illustrated in Figure 2. The two heavy lines show the function I(y) and yQ, where $Q=1.69$. The intersection of these two lines is the solution to Eq. (9). At the beginning of the iteration, y is assumed to equal 1.0, and I(y) is approximated by a line at Point A. This approximation is shown by the thin line through Point A. Equation (10) gives $y=0.467$ at the intersection of this approximation with yQ. A new line is used to approximate I(y) at Point B using the new value for y. This approximation yields Point C at $y=0.512$, and then converges on the next iteration to Point D at $y=0.513$. W is then determined using

Algorithm 5 Calculation of the global variables L_0 and A.

PROCEDURE DEFINITION OF **SetL$_0$**

This sets the global variable L_0 after γ and A have been set (see Algorithm 1).

local constants required for **SetL$_0$**:

$k \equiv \omega \cdot a \cdot B_0$

implementation of **SetL$_0$**:

$L_0 = [k/(\gamma \cdot A)]^{1/(\gamma+1)}$ *Equation 7*

PROCEDURE DEFINITION OF **SetL$_0$&A**(L, s)

This sets the gobal variables A and L_0 when γ is known (see Algorithm 1) so that $\mathcal{L}_0$ includes the point indicated by L and s. A binary search is used.

local constants required for **SetL$_0$&A**(L, s):

$k \equiv \omega \cdot a \cdot B_0$

local variables required for **SetL$_0$&A**(L, s):

ΔA, ΔL

implementation of **SetL$_0$&A**(L, s):

$A = k/(\gamma \cdot L^{\gamma+1})$ *From Equation 7; the maximum value of A is found when L is assumed to be L_0 at dusk.*

SetL$_0$

$\Delta L = L - L_{\mathcal{L}}(s)$ *from Algorithm 4.*

$\Delta A = A$ *This is the starting step size of search.*

while $abs(\Delta L) >= \delta_L$ **repeat the following loop:**

begin *while loop*

$\Delta A = \frac{1}{2}\Delta A$ *The step size is halved during each iteration.*

if $\Delta L < 0$ **then**

$A = A + \Delta A$ *A was too small.*

else

$A = A - \Delta A$ *A was too large.*

SetL$_0$

$\Delta L = L - L_{\mathcal{L}}(s)$ *from Algorithm 4.*

end *while loop*

Eq. (3). For a given L-shell and local time, y and W are first determined from Eqs. (3) and (4) using the above process, and then U is determined using Eq. (5). The given L-shell is a valid solution if the difference, ΔU, between U_M and U is zero. Algorithm 6 uses this process to solve for ΔU for a measured position and energy. Valid solutions of L for each local time give the drift path of the particle.

In summary, the drift paths of a particle are determined by calculating the three constants of motion, μ_M, J_M, U_M, for its kinetic energy and position in space using Eqs. (3), (4), and (5). Using these constants of motion, Eqs. (3) and (4) are solved simultaneously to give kinetic energy as a function of L-shell. All L-shells at a given local time for which the difference between U_M and U [Eq. (5)] is zero are on the drift path of the particle.

4. CALCULATION OF ELECTRON CUTOFF ENERGY, W_C

In a manner similar to that used to calculate drift paths, the range in energy of electrons coming from the tail that should be observed at a given position in the magnetosphere can be determined using Eqs. (3), (4), and (5). It is known that electrons

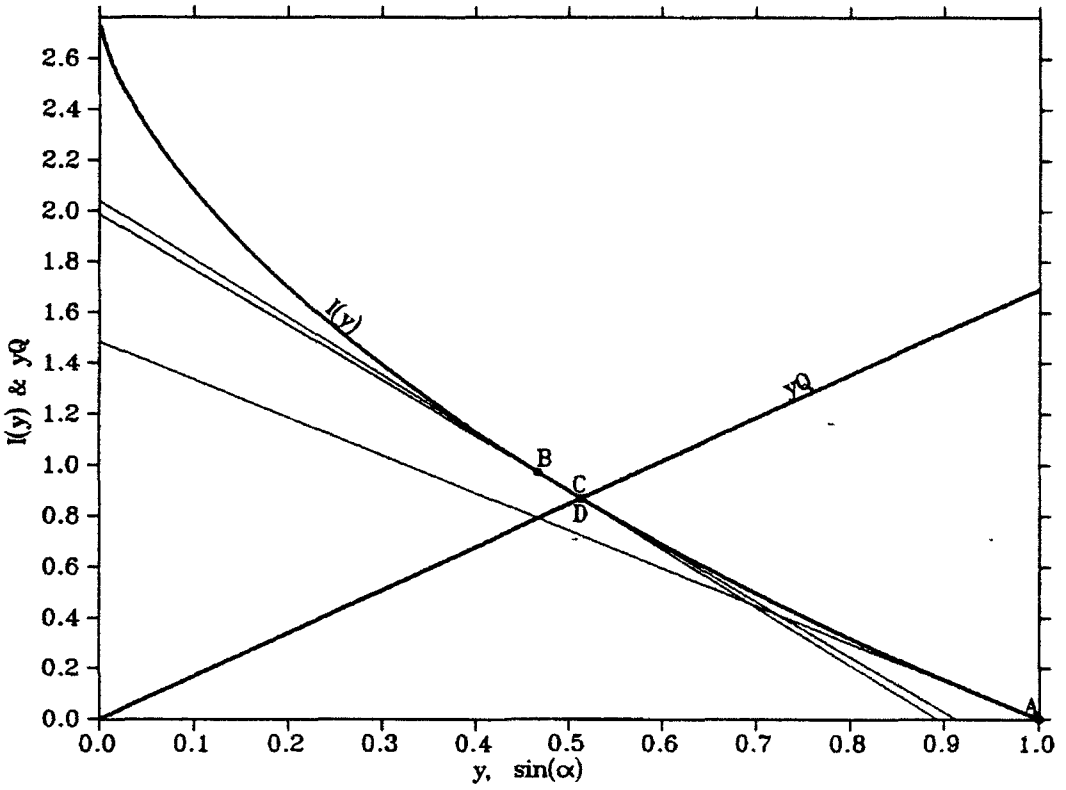

Figure 2 Example of the iterative solution of Equation 9 for $Q=1.69$. Solution starts with Point A and converges to Point D. Each thin line represents a linear approximation to I(y) at one of the points.

with $W>0$ execute a gradient curvature drift in the direction of the corotation drift. For increasing kinetic energy this gradient curvature drift comes to dominate the electric field drift, and since this drift has no radial component, the electron trajectory becomes more circular and eventually closes. For any position outside of $\mathcal{L}_0$, electrons measured with $W=0$ are on open drift paths as shown in Figure 1, and electrons measured with $W\rightarrow\infty$ are on closed circular drift paths because the magnetic drift completely dominates the electric field drift. For the position where the electron is observed, there is a cutoff energy, W_C, at which the drift trajectory changes from open to closed. Electrons convecting from the tail with energies ranging from 0 to W_C should be observed at that position. W_C is not defined for positions inside $\mathcal{L}_0$ where all electrons move on closed drift paths.

Figure 3 illustrates the electron cutoff energy, W_C. Six sets of electron drift paths in the equatorial plane are shown in this figure, and these are calculated using the method presented in Section 3 and Algorithm 6. The constants of motion are determined for electrons with one of six different values of W_M measured at the white circle with $L_M=6.0$ R_E, $y_M=0.90$, and $\sin(\phi_M)=-0.95$. The six values of W_M are given on the right side of the figure, and are labeled A to F. In this example $L_0=5$ R_E, and the shaded region is bound by $\mathcal{L}_0$. Line A shows the path for electrons with $W_M=0$. In this case there is a closed eastward path around the Earth inside of $\mathcal{L}_0$, and there is a separate

Algorithm 6 Calculation of ΔU for given constants of motion and position.

```
FUNCTION DEFINITION OF ΔU(μ, J, U, electron, L, s)
local constants required by ΔU(μ, J, U, electron, L, s):
        k ≡ B0·a²·ω
local variables required for ΔU(μ, J, U, electron, L, s):
        W, y            kinetic energy (eV) and sine of equatorial pitch angle
        al, bl          linear coefficients of Il
        i, j            integer indices of Il
        Q               of Equation 9.
implementation of ΔU(μ, J, U, electron, L, s):
        if μ = 0.0 then
                W = (J/L/I0)²           Equation 4.
        else if J = 0.0 then
                W = μ/L³                Equation 3.
        else
                begin conditional block
                i = N                   N is from Algorithm 1.
                j = 0                   this ensures that i ≠ j the first time.
                Q = J·(L/μ)^½           Equation 9.
                while i ≠ j repeat the following loop:  Check for convergence
                        begin while loop
                        j = i
                        bi = N·(Ii-Ii-1)        slope between Ii and Ii-1.
                        ai = Ii - bi·i/N        zero offset.
                        y = ai / (Q-bi)         Equation 10.
                        i = trunc(N·y) + 1      update index with new value of y.
                        end while loop
                W = μ/[(y·L)²·L]                Equation 3.
                end conditional block
        if electron then
                return value of U - W + a·A·s·L^γ - k/L  Equation 5, q=-1
        else
                return value of U - W - a·A·s·L^γ + k/L  Equation 5, q=+1
```

sunward path on the dusk side of the Earth that is open to the tail. The point of measurement is on the open path. Line B shows the path for W_M=0.6 keV electrons. Here the inner and outer paths join at a single stagnation point on the dusk meridian near 5.2 R_E, and the point of measurement is located on the open outer open path. Line C shows paths for W_M=3.8 keV electrons. Because the inner and outer paths have joined, only one path exists, and this is open to the tail and crosses the dawn-dusk meridian on the dawn side of the Earth. Line D shows the path for electrons with $W_M=W_C$. Here a closed eastward path joins at a single point on the dusk meridian near 6.5 R_E with an open sunward path. This path looks very similar to that of Line B, but here the point of measurement is on the closed inner path of Line D. Line D shows the transition trajectory between open and closed drift paths, because all electrons with $W_M<W_C$ are on open paths while higher energies, as shown by Lines E and F, place the point of measurement on closed eastward paths. In the last two cases, the open paths from the tail and the closed eastward paths are completely separate.

To calculate W_C for a measured location, the value of W_M is determined that yields a single solution of ΔU=0 on the dusk meridian as shown by Line D in Figure 3.

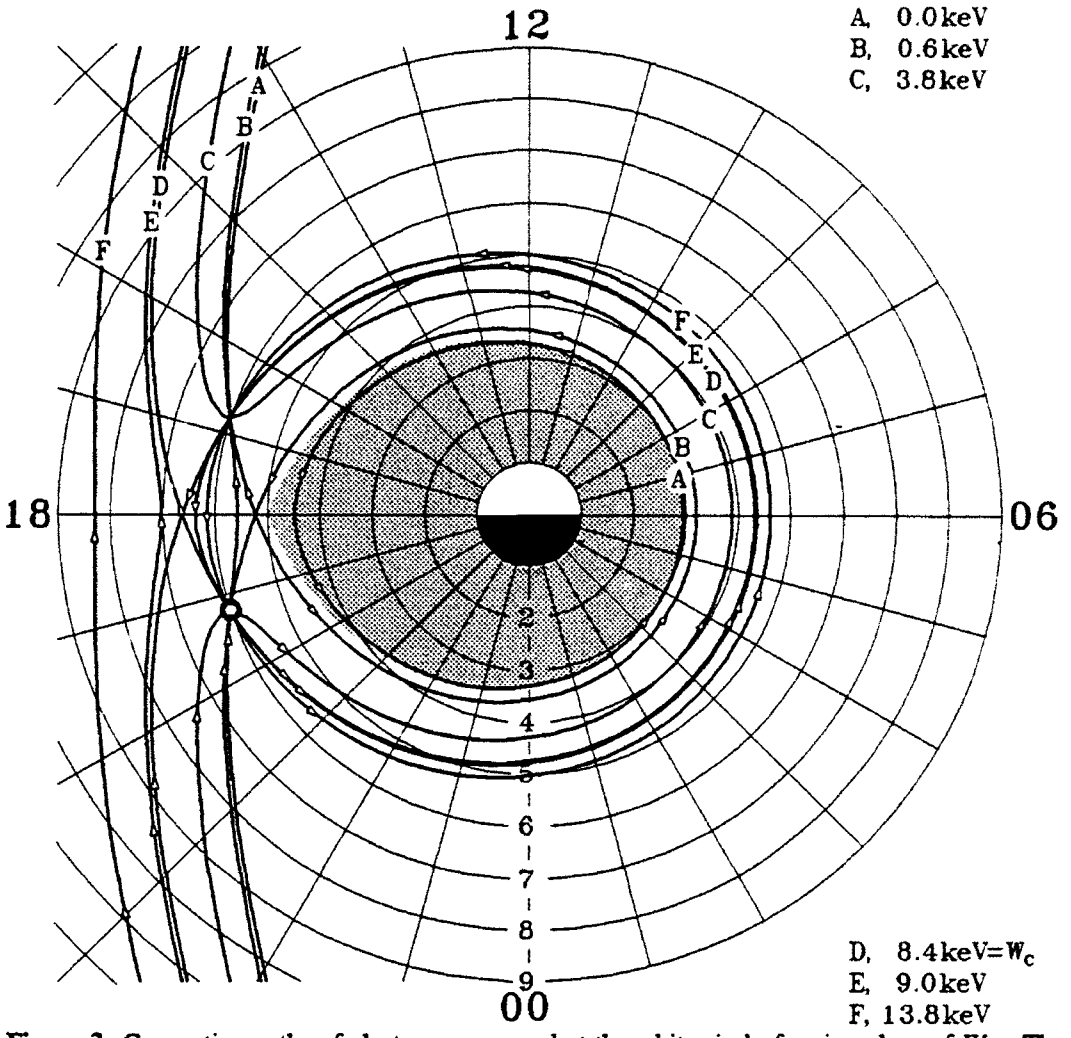

Figure 3 Convection paths of electrons measured at the white circle for six values of W_M. The shaded region is bounded by $\mathcal{L}_0$, and arrows show the direction of drift along the paths.

In Figure 4, Algorithm 6 is used to calculate ΔU, and each curve shows ΔU versus L-shell at dusk for the same six values of W_M and for the same measured location given for Figure 3. The peak values of ΔU at dusk are referred to as ΔU_P. For Curves A, E, and F, $\Delta U_P > 0$, so there are two solutions to $\Delta U = 0$ at dusk for these energies. Because there are two solutions, two separate paths are seen at dusk in Figure 3 for Lines A, E, and F. For Curve C, $\Delta U_P < 0$, so that there are no solutions to $\Delta U = 0$, and no paths are seen at dusk in Figure 3 for Line C. For Curves B and D, $\Delta U_P = 0$, so that both have exactly one solution for $\Delta U = 0$ at dusk. Both Lines B and D in Figure 3 have exactly one path on the dusk meridian, and their respective inner and outer paths join at this point. Curve D shows the proper solution for W_C, as was discussed in the previous paragraph, because it places the point of measurement on the inner path, which is closed for $W_M > W_C$ and open for $W_M < W_C$. When two values of W_M exist for which $\Delta U_P = 0$, W_C is equal to the greater value.

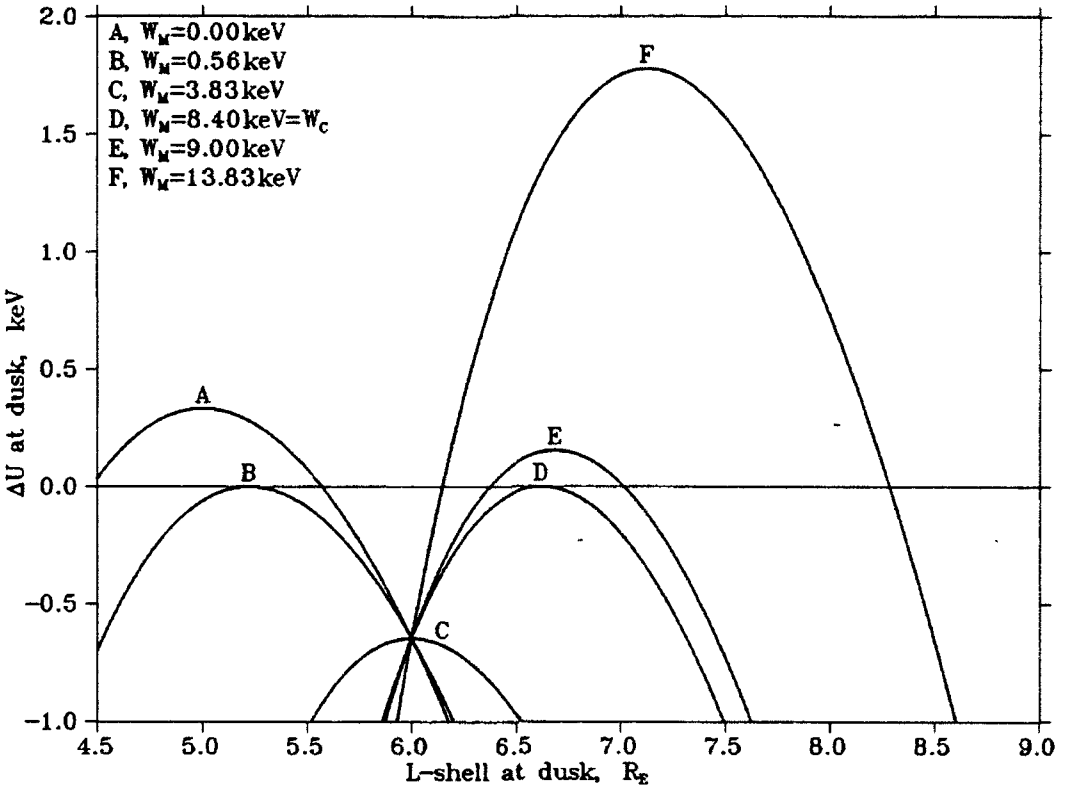

Figure 4 ΔU as a function of L-shell at dusk ($\sin(\phi)$=-1) for the same conditions, measured location, and energies as those given for Figure 3.

In order to determine the value of ΔU_P, the L-shell at dusk at which the peak occurs is identified, and this L-shell is referred to as L_P, so that $\Delta U_P = \Delta U(L_P)$. L_P occurs at the L-shell where $\partial\Delta U/\partial L = 0$ at dusk. $\Delta U = U_M - U$, and U comes from Eq. (5) with q=-1 and $\sin(\phi)$=-1, so that

$$\frac{\partial \Delta U}{\partial L}(L=L_p) = -\frac{\partial W}{\partial L}(L=L_p) - \gamma a A L_P^{\gamma-1} + B_0 a^2 \omega L_P^{-2} = 0 \qquad (11)$$

The term $\partial W/\partial L$ is derived from the simultaneous solution of Eqs. (3) and (4) as is done in Algorithm 6. From Eq. (3),

$$\frac{\partial W}{\partial L} = -3\mu_M y^{-2} L^{-4} - 2\frac{\partial y}{\partial L}\mu_M y^{-3} L^{-3} \qquad (12)$$

The $\partial y/\partial L$ term can be derived from Eq. (10) as

$$\frac{\partial y}{\partial L} = -\frac{\partial Q}{\partial L} a_l (Q - b_l)^{-2} \qquad (13)$$

and the $\partial Q/\partial L$ term can be derived from Eq. (9) as

Algorithm 7 Calculation of $\partial W/\partial L$ as a function of L-shell at dusk for a given set of constants of motion.

FUNCTION DEFINITION OF $\partial W/\partial L(\mu, J, L)$
local variables required for $\partial W/\partial L(\mu, J, L)$:

D_W	*value of $\partial W/\partial L$ returned by function.*
i, j	*integer indices to I_i.*
a_i, b_i	*linear coefficients to I_i.*
Q, D_Q, y, D_y	

implementation of $\partial W/\partial L(\mu, J, L)$:

```
if μ = 0 then
        D_W = -2[J/(L·I_o)]²/L      derived from Equation 4.
else if J = 0 then
        D_W = -3μ/L⁴                derived from Equation 3.
else
        begin conditional block
        i = N                       N is from Algorithm 1.
        j = 0                       this ensures that i≠j the first time.
        Q = J·(L/μ)^½               Equation 9.
        D_Q = ½Q/L                  Equation 14.
        while j ≠ i repeat the following loop:
                begin while loop
                j = i
                b_i = N·(I_i - I_i-1)       slope between I_i and I_i-1.
                a_i = I_i - b_i·i/N         zero offset.
                y = a_i / (Q - b_i)         Equation 10.
                i = trunc(y·N) + 1          update index with new value of y.
                end while loop
        D_y = -a_i·D_Q / (Q - b_i)²         Equation 13.
        D_W = -μ·y⁻³·L⁻⁴·(2·D_y·L + 3·y)    Equation 12.
        end conditional block
return the value of D_W
```

$$\frac{\partial Q}{\partial L} = \tfrac{1}{2} Q L^{-1} \tag{14}$$

The solution to $\partial W/\partial L$ is implemented in Algorithm 7. If either μ or J is equal to zero then $\partial W/\partial L$ is solved from either Eq. (4) or Eq. (3). Otherwise, the iterative search shown for Algorithm 6 is used to solve for y and W, and Eqs. (12), (13), and (14) are used to solve for $\partial W/\partial L$.

There is no analytic solution to Eq. (11) when Eq. (14) is substituted for $\partial W/\partial L$, so a numeric solution is used. First $\partial W/\partial L$ is approximated by a simple form which gives an analytic solution to Eq. (11). Inspection of the two extreme cases, μ_M=0 and J_M=0, of Algorithm 6 shows that $\partial W/\partial L \approx kL^{-m}$ where m ranges from 3 to 4. This is approximated by the form

$$\frac{\partial W}{\partial L} \approx c_1 L^{-2} + c_2 L^{-\gamma-3} \tag{15}$$

This form is used because it yields a quadratic equation when it is substituted into Eq.

Algorithm 8 Calculation of L_P for given values of μ and J for electrons.

FUNCTION DEFINITION OF **PeakW$_c$**(μ, J)
local constants required for **PeakW$_c$**(μ, J):
    $k \equiv B_0 \cdot a^2 \cdot \omega$
local variables required for **PeakW$_c$**(μ, J):
    L, L_1, L_2 — *These hold the current solutions of L-shell*
    D, D_1, D_2 — *These hold $\partial W/\partial L$ for the current solutions of L-shell*
    c_1, c_2, Q_A, Q_B, Q_Q
implementation of **PeakW$_c$**(μ, J):
    $L_1 = L_0$ — *Find two starting points for the iteration.*
    $D_1 = \partial W/\partial L(\mu, J, L_1)$ — *L_0 is usually within a few R_E of the final solution.*
    $L_2 = L_1 + 1.0$
    $D_2 = \partial W/\partial L(\mu, J, L_2)$
    $Q_A = -\gamma \cdot a \cdot A$ — *First coefficient of Equation 16.*
    while $abs(L_2-L_1) > \delta_L$ repeat the following loop:
        begin *while loop*
        $c_2 = (L_1^{2} \cdot D_1 - L_2^{2} \cdot D_2) / (L_1^{-\gamma+1} - L_2^{-\gamma+1})$ — *Solution to Equation 15 coefficients.*
        $c_1 = L_1^{2} \cdot D_1 - c_2 \cdot L_1^{-\gamma+1}$
        $Q_B = k - c_1$ — *Second coefficient of Equation 16.*
        $Q_Q = Q_B^{2} + 4 \cdot Q_A \cdot c_2$ — *Value inside of root in Equation 17.*
        $L = [\frac{1}{2}(-Q_B - Q_Q^{\frac{1}{2}})/Q_A]^{1/(\gamma+1)}$ — *Equation 17 yields better value for L.*
        $D = \partial W/\partial L(\mu, J, L)$ — *New value for $\partial W/\partial L$ is computed.*
        if $abs(L - L_1) < abs(L - L_2)$ then — *Replace whichever solution is farthest from new solution.*
            begin *conditional block*
            $L_2 = L$
            $D_2 = D$
            end *conditional block*
        else
            begin *conditional block*
            $L_1 = L$
            $D_1 = D$
            end *conditional block*
        end *while loop*
    return value of L

(11). Substitution of Eq. (15) into Eq. (11), and multiplying both sides by $L^{\gamma+3}$ gives

$$0 \approx -\gamma a A L_P^{2\gamma+2} + (B_0 a^2 \omega - c_1) L_P^{\gamma+1} - c_2 \tag{16}$$

The solution of interest is

$$L_P \approx \left[\frac{-Q_B - (Q_B^2 - 4 Q_A Q_C)^{1/2}}{2 Q_A} \right]^{1/(\gamma+1)} \tag{17}$$

where $Q_A = -\gamma a A$, $Q_B = B_0 a^2 \omega - c_1$, and $Q_C = -c_2$. The values of c_1 and c_2 are first determined from two points at $L = L_0$ and $L = L_0 + 1$. An estimate of L_P is determined using Eq. (17), and this new value is used to replace the initial estimated value of L-shell farthest from the new estimate. New values for c_1 and c_2 are determined which then give a better estimate of L_P. This process is repeated until it converges to a solution, usually in four to five iterations. Algorithm 8 shows this method of determining L_P.

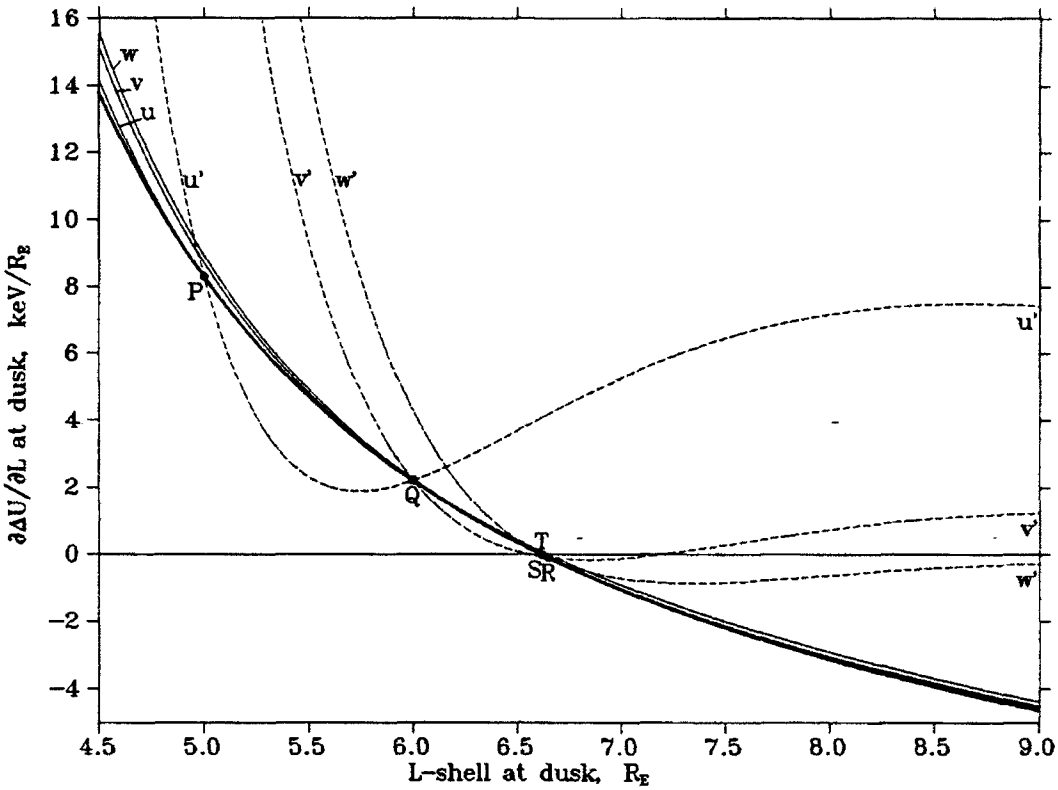

Figure 5 Slope of Curve D in Figure 4. The bold line is the actual slope, and the thin solid lines are approximations using Eq. (15). The dashed lines exaggerate the error between the approximations and actual slope by a factor of 50.

Figure 5 illustrates Algorithm 8 for the solution of L_P for the case $W_M=W_C$, Curve D of Figure 4. The bold line shows $\partial\Delta U/\partial L$ as a function of L-shell at dusk. L_P is located where this line crosses zero (Point T). Points P and Q at $L=L_0$ and $L=L_0+1$ are used to determine initial values for c_1 and c_2 [Eq. (15)]. Line u, which is a thin solid line, shows the approximation to $\partial\Delta U/\partial L$ by using Eq. (15). Because the approximation is very close to the actual solution, Line u', which is a thin dashed line, shows the error between the approximation and the actual solution exaggerated by a factor of 50. Equation (17) identifies the L-shell of the zero intersect of Line u at Point R. The second iteration uses Points Q and R to determine c_1 and c_2. This approximation is shown by Line v with the exaggerated error shown by Line v'. Here the approximation is more accurate near the solution. Point S, which is the zero intercept of Line v, is used with Point R for the final iteration shown by Line w. Line w' shows that the approximation is very good near the solution shown by Point T. The iteration is stopped here because the difference between the Points S and T is sufficiently small.

Because there are potentially two values of W_M for which $\Delta U_P=0$, as shown by Curves B and D in Figure 4, it is necessary to identify a lower limit to W_M which is always larger than the smaller solution to $\Delta U_P=0$ and is less than or equal to the larger, correct solution. In Figure 4, all of the curves have the same value of ΔU at $L=6.0$ R_E because this is the value of L_M. When $L=L_M$, conservation of the first two adiabatic

invariants [Eqs. (3) and (4)] requires that $W=W_M$, and $y=y_M$. Substituting Eq. (5) into $\Delta U=U_M-U$ yields

$$\Delta U(L=L_M) = -aAL_M^{\gamma}[1+\sin(\phi_M)] \tag{18}$$

and this shows that $\Delta U(L=L_M)\leq 0$. As can be seen by looking at Curve C, $\Delta U(L=L_M)$ is the minimum possible value of ΔU_P. The value of W_M that gives $\Delta U_P=\Delta U(L=L_M)$ is referred to as W_0, and is obtained by setting $\partial\Delta U/\partial L(L=L_M)$ to zero. Since U_M is a constant, the equation is

$$\frac{\partial \Delta U}{\partial L}(L=L_M) = -\frac{\partial W}{\partial L}(L=L_M) - \gamma aAL_M^{\gamma-1} + B_0 a^2 \omega L_M^{-2} = 0 \tag{19}$$

For two different electrons, labeled 1 and 2, if $L_1=L_2$ and $y_1=y_2$ then Eqs. (3) and (4) require that $\mu_2 W_1=\mu_1 W_2$ and $J_2^2 W_1=J_1^2 W_2$ respectively. With these requirements, Eq. (9) shows $Q_2=Q_1$, Eq. (14) shows $\partial Q_2/\partial L=\partial Q_1/\partial L$, and Eq. (13) shows $\partial y_2/\partial L=\partial y_1/\partial L$. Equation (12) then shows that

$$W_2 = W_1 \frac{\partial W_2}{\partial L}\left[\frac{\partial W_1}{\partial L}\right]^{-1} \tag{20}$$

To solve for W_0, $\partial W/\partial L(L=L_M)$ from Eq. (19) is substituted into $\partial W_2/\partial L$ in Eq. (20). Any energy, W_{any}, can be used for W_1 provided that $\partial W_1/\partial L$ uses the constants of motion from $L=L_M$, $y=y_M$, $\phi=\phi_M$, and $W=W_{any}$. This gives

$$W_0 = W_{any}\left(B_0 \omega a^2 L_M^{-2} - \gamma aAL_M^{\gamma-1}\right)\left[\frac{\partial W}{\partial L}(W=W_{any}, L=L_M)\right]^{-1} \tag{21}$$

Substitution of Eq. (7) into Eq. (21) shows that $W_0>0$ for $L_M>L_0$, and $W_0<0$ for $L_M<L_0$. When $W_0>0$, two values of W_M may exist for which $\Delta U_P=0$, and W_0 is between these two values. In Figure 4, W_0 is the energy used for Curve C, and Curves B and D use the lower and upper values of W_M for which $\Delta U_P=0$. When $W_0\leq 0$, only one solution can exist because kinetic energy cannot be negative.

W_C is determined by identifying the value of $W_M>W_0$ that gives $\Delta U_P=0$. Algorithm 9 shows the implementation of the iterative search used to find W_C for a position given as $y=y_M$, $L=L_M$, and $\sin(\phi)=s_M$. If $L_M<L_0$, then the location L_M, s_M is outside of $\mathcal{L}_0$ if U for $W_M=0$ electrons is less than U of $\mathcal{L}_0$. This can be seen in Figure 1 in which the contour lines show negative U because kinetic energy is zero and q is negative. If the measured position is inside of $\mathcal{L}_0$, then W_C is given the value of -1 to indicate that W_C is not defined. The initial lower value of W_M for the search is given by Eq. (21). This equation gives a negative solution if $L_M<L_0$, and for these cases an initial lower value of $W_M=0$ is used. The initial upper value is chosen arbitrarily to be 10 keV greater than the lower value. A third point is picked by assuming the first two points lie on a parabola, and the slope of the parabola is zero at the lower point. If $W_0<0$, a third point is simply picked halfway between the first two points. A parabola is then used to

Algorithm 9 Calculation of electron cutoff energy, W_C, for a position given by L, y, and $\sin(\phi)$.

FUNCTION DEFINITION OF $W_c(y, L, s)$
local constants required for $W_c(y, L, s)$:
$k \equiv B_0 \cdot \omega \cdot a^2$
local variables required for $W_c(y, L, s)$:
$U_0, \mu_1, J_1, W_0, W_1, W_2, \Delta U_0, \Delta U_1, \Delta U_2, Q_A, Q_B, Q_C$
implementation of $W_c(y, L, s)$:
$\mu_1 = \mu(y, 1, L)$ *Value of μ at y,L,s if $W = 1$ eV; $\mu = \mu_1 \cdot W$ Eqn 3*
$J_1 = J(y, 1, L)$ *Value of J at y,L,s if $W = 1$ eV; $J = J_1 \cdot W^{\frac{1}{2}}$ Eqn 4*
$U_0 = U(\text{true}, 0, L, s)$ *Value of U at y,L,s if $W = 0$ eV; $U = U_0 + W$ Eqn 5*
if $(L < L_0)$ and $[\Delta U(0, 0, U_0, \text{true}, L_0, -1) > 0]$ then *satellite is inside of $\mathcal{L}_0$*
return value of -1 and exit function *-1 indicates that W_c does not exist*
Equation 21 finds initial starting point of search.
if $L > L_0$ then
$W_0 = W_{step} \cdot (k/L^2 - \gamma \cdot a \cdot A \cdot L^{r-1}) \,/\, \partial W / \partial L(\mu_1 \cdot W_{step}, J_1 \cdot W_{step}^{\frac{1}{2}}, L)$
else
$W_0 = 0$ *Equation 21 returns a negative value so use $W_0 = 0$*
$\Delta U_0 = \Delta U(\mu_1 \cdot W_0, J_1 \cdot W_0^{\frac{1}{2}}, U_0 + W_0, \text{true}, \text{PeakW}_c(\mu_1 \cdot W_0, J_1 \cdot W_0^{\frac{1}{2}}), -1)$ ★
The second starting point is offset from the first by W_{step}.
$W_1 = W_0 + W_{step}$
$\Delta U_1 = \Delta U(\mu_1 \cdot W_1, J_1 \cdot W_1^{\frac{1}{2}}, U_0 + W_1, \text{true}, \text{PeakW}_c(\mu_1 \cdot W_1, J_1 \cdot W_1^{\frac{1}{2}}), -1)$ ★
A parabolic approximation is used to find the third point. It uses the points W_0 and W_1, and assumes the slope at W_0 is zero.
if $W_0 = 0$ then
$W_2 = \frac{1}{2} W_1$ *Slope at W_0 is not zero if $W_0 = 0$; use midpoint.*
else
$W_2 = W_0 + W_{step} \cdot [\Delta U_0 / (\Delta U_0 - \Delta U_1)]^{\frac{1}{2}}$ *This is zero intercept of parabola.*
$\Delta U_2 = \Delta U(\mu_1 \cdot W_2, J_1 \cdot W_2^{\frac{1}{2}}, U_0 + W_2, \text{true}, \text{PeakW}_c(\mu_1 \cdot W_2, J_1 \cdot W_2^{\frac{1}{2}}), -1)$ ★
Reorder W_0, W_1, and W_2 so that $|\Delta U_0| < |\Delta U_1| < |\Delta U_2|$
if $\text{abs}(\Delta U_1) < \text{abs}(\Delta U_0)$ then
swap values of ΔU_1 with ΔU_0 and W_1 with W_0
if $\text{abs}(\Delta U_2) < \text{abs}(\Delta U_1)$ then
swap values of ΔU_2 with ΔU_1 and W_2 with W_1
if $\text{abs}(\Delta U_1) < \text{abs}(\Delta U_0)$ then
swap values of ΔU_1 with ΔU_0 and W_1 with W_0
while $\text{abs}(W_1 - W_0) > \delta_W \cdot (W_0 + W_1)$ repeat following loop:
begin *while loop*
$Q_A = [\Delta U_0 \cdot (W_2 - W_1) + \Delta U_1 \cdot (W_0 - W_2) + \Delta U_2 \cdot (W_1 - W_0)] \,/\, [W_0^2 \cdot (W_2 - W_1) + W_1^2 \cdot (W_0 - W_2) + W_2^2 \cdot (W_1 - W_0)]$
$Q_B = [\Delta U_0 - \Delta U_1 - Q_A \cdot (W_0^2 - W_1^2)] \,/\, (W_0 - W_1)$
$Q_C = \Delta U_0 - W_0 \cdot (Q_B + Q_A \cdot W_0)$
$\Delta U_2 = \Delta U_1$ *Shift point 1 to point 2*
$W_2 = W_1$ *and point 0 to point 1,*
$\Delta U_1 = \Delta U_0$ *and find new point 0.*
$W_1 = W_0$
$W_0 = \frac{1}{2} \cdot [-Q_B + (Q_B^2 - 4 \cdot Q_A \cdot Q_C)^{\frac{1}{2}}] \,/\, Q_A$ *Quadratic Formula*
$\Delta U_0 = \Delta U(\mu_1 \cdot W_0, J_1 \cdot W_0^{\frac{1}{2}}, U_0 + W_0, \text{true}, \text{PeakW}_c(\mu_1 \cdot W_0, J_1 \cdot W_0^{\frac{1}{2}}), -1)$ ★
end *while loop*
return value of W_0

★ *These lines can be made more efficient by calculating $\mu_1 \cdot W_n$ and $J_1 \cdot W_n^{\frac{1}{2}}$ only once for each line instead of twice.*

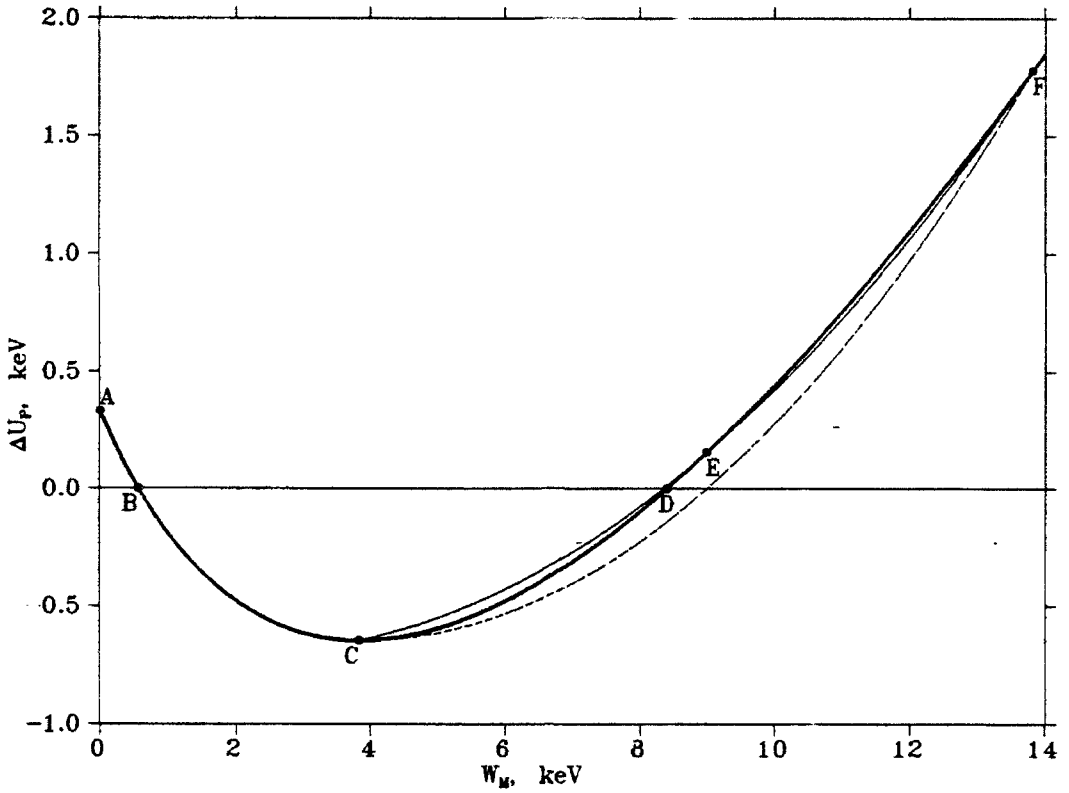

Figure 6 Relationship between ΔU_P and W_M for the conditions given for Figure 4. This illustrates the solution for W_C.

approximate the relationship between ΔU_P and W_M using the three points, and it is used to solve for a new value of W_M. The point that is farthest from $\Delta U_P=0$ is replaced by the new solution for W_M in the next iteration. The iteration is continued until the value of $W_C=W_M$ is known to sufficient accuracy, usually in about three iterations.

Figure 6 illustrates the solution for W_C for the conditions given for Figures 3 and 4, and Points A through F have the same energy as do those in the previous figures. The x axis shows W_M, the y axis shows ΔU_P, and the dark curve shows the relationship between the two. The initial lower boundary at Point C is identified using Eq. (21), and the initial upper boundary at Point F is found by adding 10 keV to the energy of Point C. Point E is found using the zero intercept of the parabola formed from Points C and F with a slope of zero at Point C (shown by thin dotted line). The zero intercept of the parabola formed from Points C, E and F (thin solid line) is very close to the true solution shown by Point D. The process converges to Point D on the next iteration.

5. CALCULATION OF ION LOWER CUTOFF ENERGY, W_L

Ions move in a more complex manner than do electrons because the magnetic gradient and curvature drift of ions is westward which is counter to that of the corotation electric field drift. Ions with zero kinetic energy experience no gradient and curvature

drift, and so move identically to electrons with zero kinetic energy. Therefore, an ion inside of $\mathcal{L}_0$ with $W=0$ moves eastward on a closed drift path. As $W \to \infty$, the gradient curvature drift completely dominates the electric field drift so that the ion moves westward on a closed circular drift path. The drift paths for intermediate kinetic energies transition from closed eastward paths to closed westward paths, and many of these paths are open to the tail. The bounding limits to the range of kinetic energy open to the tail are W_L for the lower bound and W_H for the upper bound. Ions with $W < W_L$ move on closed eastward drift paths, and ions with $W > W_H$ move on closed westward drift paths. W_L is not defined for positions outside of $\mathcal{L}_0$ because here no ions can move on closed eastward drift paths. The two ion cutoff energies are discussed separately, W_L in this section, and W_H in Section 6.

Figure 7 illustrates the ion lower cutoff energy, W_L. Four sets of ion drift paths in the equatorial plane are shown in this figure; they are calculated using the method

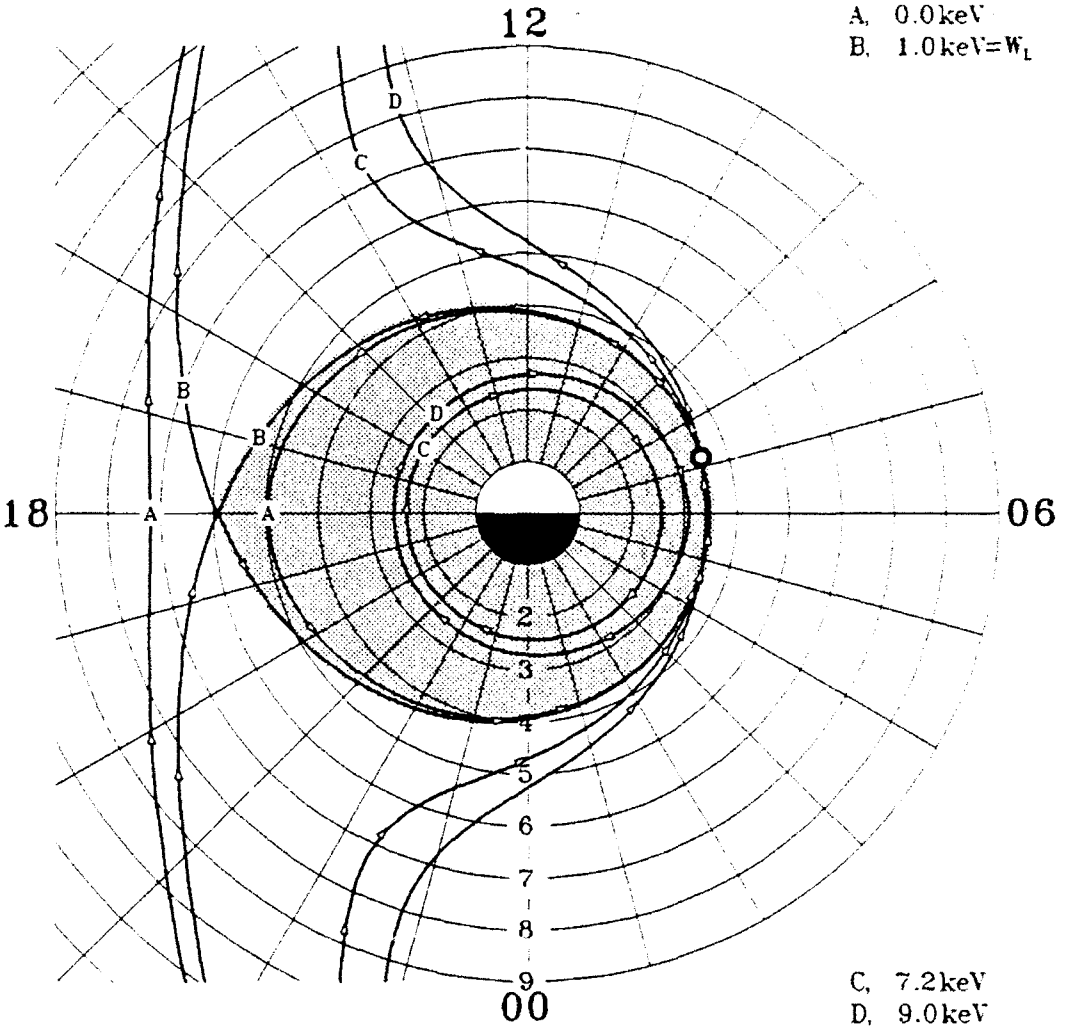

Figure 7 Convection paths of singly charged ions measured at the white circle for four values of W_M. The shaded region is bounded by $\mathcal{L}_0$, and arrows show the direction of drift along the paths.

presented in Section 3 and Algorithm 6. The constants of motion are determined for ions with one of four different values of W_M measured at the white circle with L_M=3.5 R_E, y_M=0.90, and sin(ϕ_M)=0.95. In each case, $W_M < W_H$. The four values of W_M are given on the right side of the figure and are labeled A to D. In this example L_0=6 R_E, and the shaded region is bounded by $\mathcal{L}_0$. Line A shows the path for ions with W_M=0. For these ions, there is a closed eastward path around the Earth inside of $\mathcal{L}_0$, and there is a separate sunward path that is open to the tail on the dusk side of the Earth. The point of measurement is on the closed path whereas it is on the open path for electrons with W_M=0. Line B shows the path for ions with $W_M = W_L$. Here a closed eastward path joins at a single point on the dusk meridian with an open sunward path. This path looks very similar to that for electrons with $W_M = W_L$ except that the paths join inside of $\mathcal{L}_0$. This is the transition trajectory between open and closed drift paths, because all ions with $W_M < W_L$ are on closed paths while higher energies, as shown by Lines C and D, place the point of measurement on paths open to the tail. In the last two cases, the open paths from the tail and the closed eastward paths join to form a single path that crosses the dawn-dusk meridian on the dawn side of the Earth. Lines C and D also show two closed westward drift paths inside of the point of measurement. Electron drift paths have no equivalent to these paths because the electron gradient curvature drift is eastward.

W_L is calculated in a manner similar to that of W_C. In Figure 8, Algorithm 6 is used to calculate ΔU, and four curves show ΔU versus L-shell at dusk for the same four values of W_M and for the same measured location given for Figure 7. Comparison of this

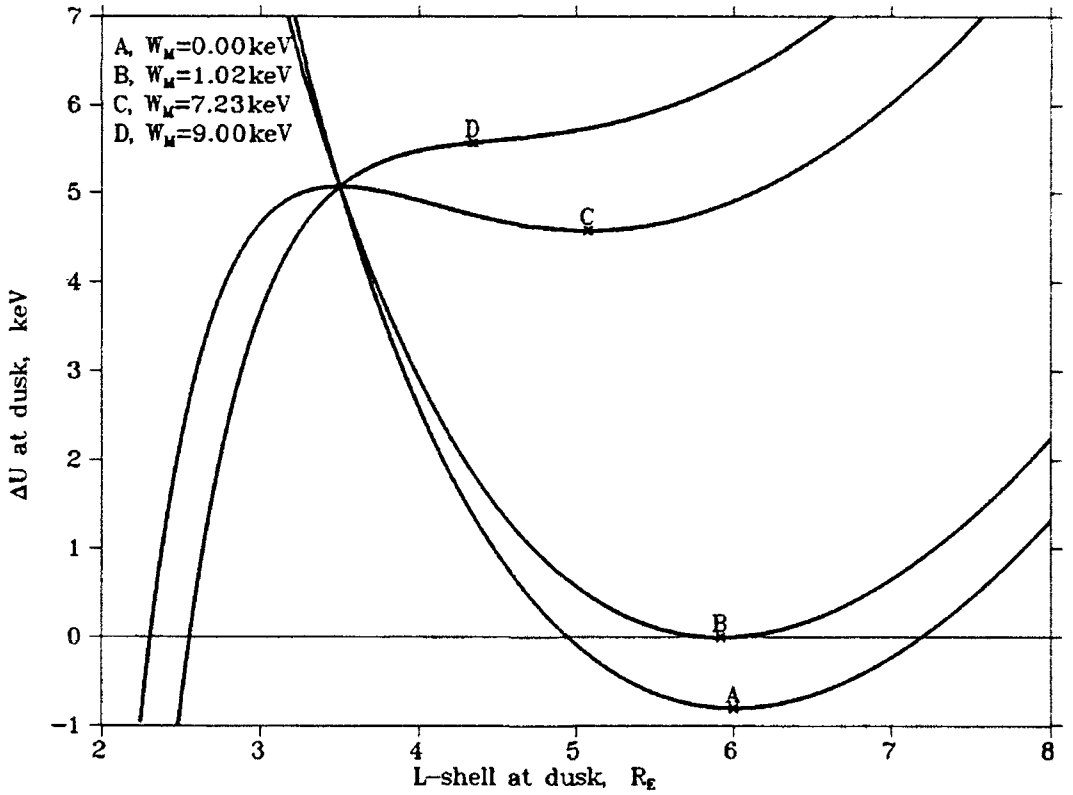

Figure 8 ΔU as a function of L-shell at dusk (sin(ϕ)=-1) for the same conditions, measured location, and energies as those given for Figure 7. The crosses mark the location of ΔU_P.

figure to Figure 4 shows the more complex nature of the ions. In Figure 4 there is one peak for each electron energy. In Figure 8, peaks can be seen in Curves A, B, and C at the crosses, but the peaks are negative, and a peak does not exist for Curve D. Also, Curves C and D show an extra solution to $\Delta U=0$ at L-shells between 2 and 3 R_E. These two inner solutions form the closed westward drift paths for Lines C and D of Figure 7. The peak values of ΔU at dusk are referred to as ΔU_P. In cases where a peak does not exist, ΔU_P is defined at the point were the slope minimizes as is shown by the cross on Curve D. For Curve A, $\Delta U_P<0$, so there are two solutions to $\Delta U=0$ at dusk for this energy. Because there are two solutions, there are two separate paths seen at dusk in Figure 7 for Line A. For Curves C and D, $\Delta U_P>0$, so that there are no solutions other than that for the inner closed westward drift path, and only this path is seen at dusk in Figure 7 for Lines C and D. $\Delta U_P=0$ for Curve B, so Line B of Figure 7 has exactly one

Algorithm 10 Calculation of L_P at dusk for given values of μ and J for ions.

```
FUNCTION DEFINITION OF PeakW_L(μ, J)
local constants required for PeakW_L(μ, J):
        k ≡ -B_0·a^2·ω
local variables required for PeakW_L(μ, J):
        L, L_1, L_2              These hold the current solutions of L-shell
        D, D_1, D_2              These hold ∂W/∂L for the current solutions of L-shell
        c_1, c_2, Q_A, Q_B, Q_Q
implementation of PeakW_L(μ, J):
        L_1 = L_0                        Find two starting points for the iteration.
        D_1 = ∂W/∂L(μ, J, L_1)           L_0 is usually within a few R_E of the final solution.
        L_2 = L_1 - 1.0
        D_2 = ∂W/∂L(μ, J, L_2)
        Q_A = γ·a·A                      First coefficient for Equation 23.
        while abs(L_2-L_1) > δ_L repeat the following loop:
                begin while loop
                c_2 = (L_1^2·D_1 - L_2^2·D_2) / (L_1^-γ-1 - L_2^-γ-1)   Solution to Equation 15
                c_1 = L_1^2·D_1 - c_2·L_1^-γ-1                          coefficients.
                Q_B = k - c_1                    Second coefficient for Equation 23.
                Q_Q = Q_B^2 + 4·Q_A·c_2          Value inside of root in Equation 23.
                if Q_Q<0 then                    If no peak is found then search for
                        Q_Q=0                            minimum slope.
                L = [½(-Q_B + Q_Q^½)/Q_A]^1/(γ+1)   Equation 23 yields better value for L.
                D = ∂W/∂L(μ, J, L)               New value for ∂W/∂L is computed.
                if abs(L - L_1) < abs(L - L_2) then      Replace whichever solution is
                        begin conditional block          farthest from new solution.
                        L_2 = L
                        D_2 = D
                        end conditional block
                else
                        begin conditional block
                        L_1 = L
                        D_1 = D
                        end conditional block
                end while loop
        return value of L
```

solution for $\Delta U=0$ at dusk, and the inner and outer paths join at this point.

To determine the value of ΔU_P, the L-shell at dusk at which the peak occurs is identified. This L-shell is referred to as L_P, so that $\Delta U_P=\Delta U(L_P)$. L_P occurs at the L-shell where $\partial\Delta U/\partial L=0$ at dusk. $\Delta U=U_M-U$, and U comes from Eq. (5) with $q=1$ and $\sin(\phi)=-1$, so that

$$\frac{\partial \Delta U}{\partial L}(L=L_P) = -\frac{\partial W}{\partial L}(L=L_P) + \gamma a A L_P^{\gamma-1} - B_0 a^2 \omega L_P^{-2} = 0 \qquad (22)$$

This solution is identical to Eq. (11) except for sign changes in the second and third terms. It is solved iteratively as is Eq. (11) by using Eq. (15) except that the solution of interest is

$$L_P \approx \left[\frac{-Q_B + (Q_B^2 - 4 Q_A Q_C)^{1/2}}{2 Q_A} \right]^{1/(\gamma+1)} \qquad (23)$$

where $Q_A=\gamma aA$, $Q_B=-B_0a^2\omega-c_1$, and $Q_C=-c_2$. The values of c_1 and c_2 of Eq. (15) are first determined from initial estimates of $L=L_0$ and $L=L_0$-1. An estimate of L_P is determined using Eq. (23), and this new value is used to replace the initial estimated value of L-shell farthest from the new estimate. New values for c_1 and c_2 are determined giving a better estimate of L_P. If no peak is found, such as in the case shown by Curve D of Figure 8, the term in Eq. (23) inside of the radical is set to zero, so that Eq. (23) identifies the L-shell of minimum slope. This process is repeated until it converges to a solution, usually in four to five iterations. Algorithm 10 shows this method of determining L_P.

Figure 9 illustrates Algorithm 10 for the solution of L_P for the case $W_M=W_L$, Curve B of Figure 8. The bold line shows $\partial\Delta U/\partial L$ as a function of L-shell at dusk. L_P is located where this line crosses zero (Point S). Points P and Q at $L=L_0$ and $L=L_0$-1 are used to determine initial values for c_1 and c_2 [Eq. (15)]. Line u, which is a thin solid line, shows the approximation to $\partial\Delta U/\partial L$ using Eq. (15). Because the approximation is very close to the actual solution, Line u', which is a thin dashed line, is shown with the error between the approximation and the actual solution exaggerated by a factor of 500. Equation (23) identifies the L-shell of the zero intersect of Line u at Point R. The second and final iteration uses Points P and R to determine c_1 and c_2. This approximation is shown by Line v with the exaggerated error shown by Line v'. Point S is the zero intercept of Line v. The iteration is stopped here because the difference between the Points R and S is sufficiently small.

W_L is determined by identifying the value of W_M which gives $\Delta U_P=0$. The initial value used to determine W_L is found in a manner similar to that for W_C given by Eq. (21). Because the sign of q is changed, there are sign changes in Eq. (21), giving

$$W_0 = W_{any}\left(\gamma a A L_M^{\gamma-1} - B_0 \omega a^2 L_M^{-2}\right)\left[\frac{\partial W}{\partial L}(W=W_{any}, L=L_M)\right]^{-1} \qquad (24)$$

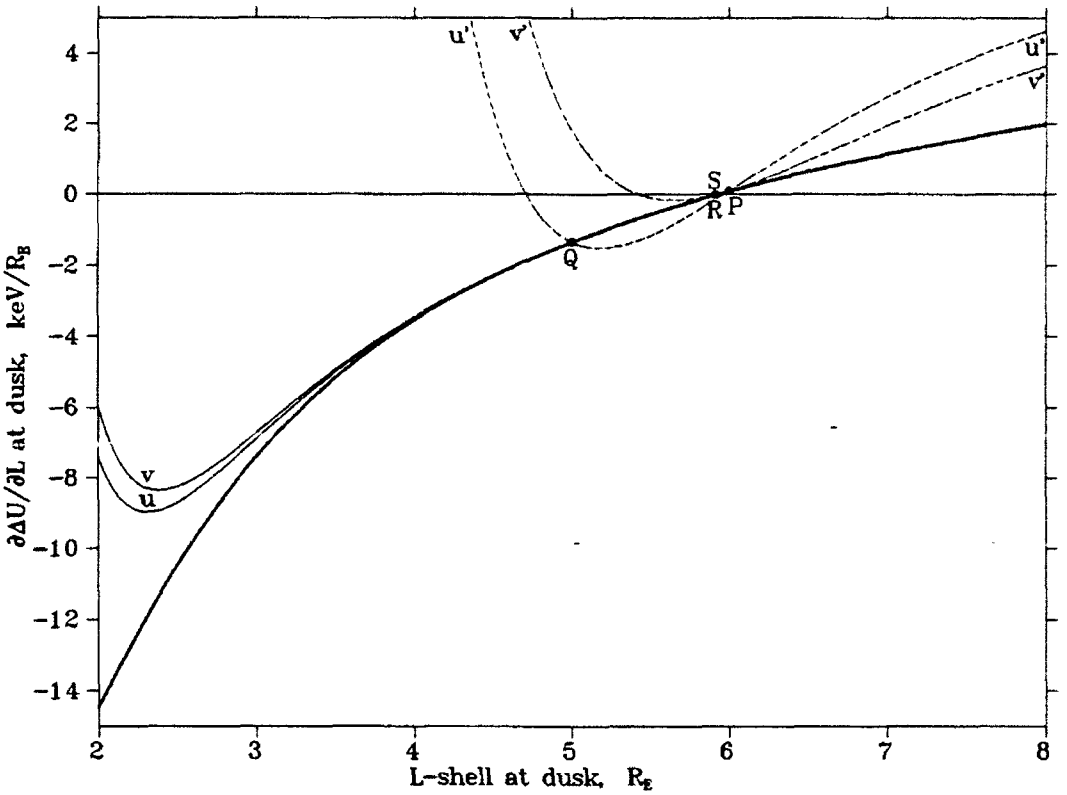

Figure 9 Slope of Curve B in Figure 8. The bold line is the actual slope, and the thin solid lines are approximations using Eq. (15). The dashed lines exaggerate the error between the approximations and actual slope by a factor of 500.

Algorithm 11 shows the implementation of the iterative search used to find W_L for a position given as $y=y_M$, $L=L_M$, and $\sin(\phi)=s_M$. If $L_M<L_0$ then the location, L_M, s_M, is outside of $\mathcal{L}_0$ if U for $W_M=0$ ions is greater than U of $\mathcal{L}_0$. This can be seen in Figure 1 where the contour lines are equal to U since q is positive. If the measured position is outside of $\mathcal{L}_0$, then W_L is given the value of -1 to indicate that W_L is not defined. The initial upper value of W_M for the search is given by Eq. (24). $L<L_0$ because W_L is only defined for positions inside of $\mathcal{L}_0$. Substitution of Eq. (7) into Eq. (24) shows that Eq. (24) gives a positive result when $L<L_0$. The initial lower value is set to zero. A line is used to approximate the relationship between ΔU_P and W_M using two points and is used to solve for a new value of W_M. The point farthest from $\Delta U_P=0$ is replaced by the new solution for W_M for the next iteration. The iteration is continued until the value of $W_L=W_M$ is known to sufficient accuracy, usually in about three iterations.

Figure 10 illustrates the solution for W_L for the conditions given for Figures 7 and 8, and Points A through D have the same energy as do those in the previous figures. The x axis shows W_M, the y axis shows ΔU_P, and the dark curve shows the relationship between the two. The curve is shown as a dotted line on the right side of the figure where a peak does not exist at ΔU_P such as for that shown by Curve D in Figure 8. The initial upper boundary at Point C is identified using Eq. (24), and the initial lower boundary at Point A is at $W_M=0$. The thin solid line connecting Points A and C shows

Algorithm 11 Calculation of ion lower cutoff energy ,W_L, for a position given by L, y, and $\sin(\phi)$.

FUNCTION DEFINITION OF $W_L(y, L, s)$
local constants required for $W_L(y, L, s)$:
$k \equiv B_0 \cdot \omega \cdot a^2$
local variables required for $W_L(y, L, s)$:
$U_0, \mu_1, J_1, W, W_0, W_1, \Delta U, \Delta U_0, \Delta U_1$
implementation of $W_L(y, L, s)$:
$\mu_1 = \mu(y, 1, L)$ *Value of μ at y,L,s if W=1 eV; $\mu = \mu_1 \cdot W$* *Eqn 3*
$J_1 = J(y, 1, L)$ *Value of J at y,L,s if W=1 eV; $J = J_1 \cdot W^{½}$* *Eqn 4*
$U_0 = U(\text{false}, 0, L, s)$ *Value of U at y,L,s if W=0 eV; $U = U_0 + W$* *Eqn 5*
$W_0 = 0$
$\Delta U_0 = \Delta U(0, 0, U_0, \text{false}, L_0, -1)$
if $(L > L_0)$ or $[\Delta U_0 > 0]$ then *satellite is outside of $\mathcal{L}_0$*
return value of -1 and exit function *-1 indicates that W_L does not exist*
$W_1 = W_{step} \cdot (\gamma \cdot a \cdot A \cdot L^{r-1} - k/L^2) \,/\, \partial W/\partial L(\mu_1 \cdot W_{step}, J_1 \cdot W_{step}^{½}, L)$ *Equation 24*
$\Delta U_1 = \Delta U(\mu_1 \cdot W_1, J_1 \cdot W_1^{½}, U_0 + W_1, \text{false}, \text{PeakW}_L(\mu_1 \cdot W_1, J_1 \cdot W_1^{½}), -1)$ ★
while $\text{abs}(W_1 - W_0) > \delta_W \cdot (W_0 + W_1)$ repeat following loop:
begin *while loop*
$W = W_0 - (W_1 - W_0)/(\Delta U_1 - \Delta U_0) \cdot \Delta U$
$\Delta U = \Delta U(\mu_1 \cdot W, J_1 \cdot W^{½}, U_0 + W, \text{false}, \text{PeakW}_L(\mu_1 \cdot W, J_1 \cdot W^{½}), -1)$ ★
if $\text{abs}(\Delta U_1) < \text{abs}(\Delta U_0)$ then
begin *conditional block*
$W_0 = W$
$\Delta U_0 = \Delta U$
end *conditional block*
else
begin *conditional block*
$W_1 = W$
$\Delta U_1 = \Delta U$
end *conditional block*
end *while loop*
return value of W

★ *These lines can be made more efficient by calculating $\mu_1 \cdot W_n$ and $J_1 \cdot W_n^{½}$ only once for each line instead of twice.*

---

the linear approximation to the relationship. The zero intercept of this approximation is very close the actual solution, shown by Point B. The process converges to Point B in one to two more iterations.

6. CALCULATION OF ION UPPER CUTOFF ENERGY, W_H

Figure 11 illustrates the ion upper cutoff energy, W_H. Six sets of ion drift paths in the equatorial plane are shown in this figure, and these are calculated using the method presented in Section 3 and Algorithm 6. The constants of motion are determined for ions with one of six different values of W_M measured at the white circle with L_M=3.5 R_E, y_M=0.90, and $\sin(\phi_M)$=0.95. In each case, $W_M > W_L$. The six values of W_M are given on the right side of the figure and are labeled A to G. The letter C is omitted so that the energies shown in this figure will match the energies used in following figures. In this example L_0=6 R_E, and the shaded region is bounded by $\mathcal{L}_0$. Line A shows the path for

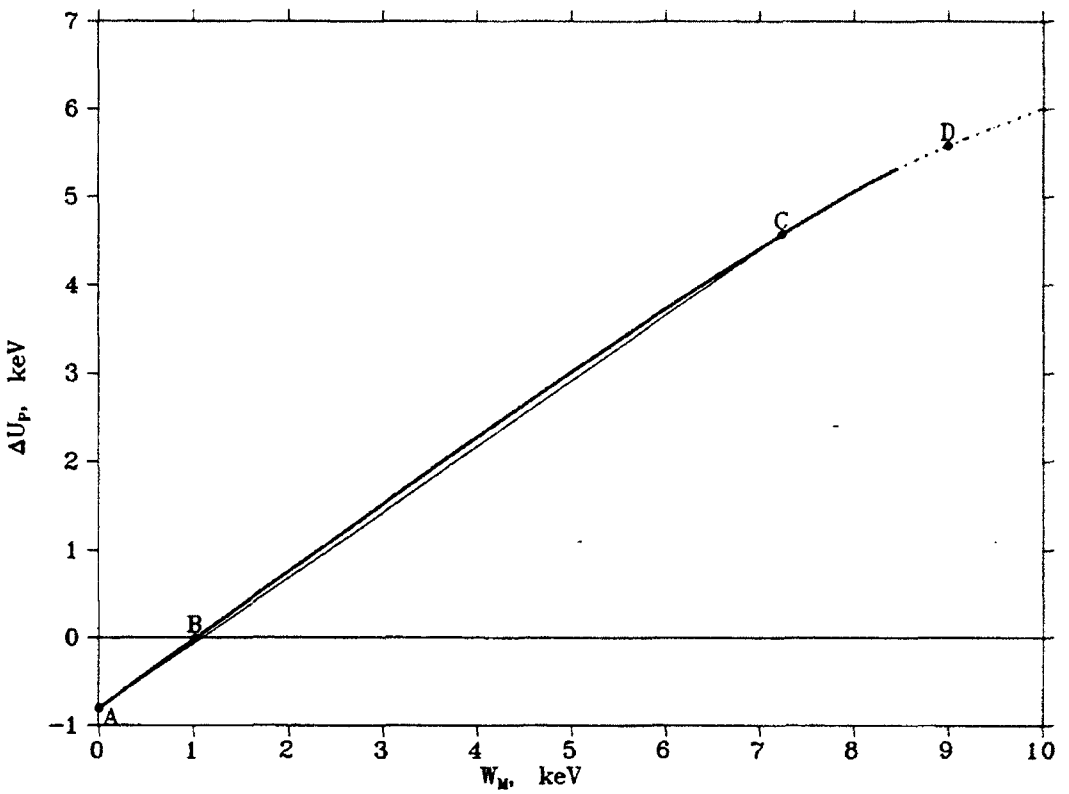

Figure 10 Relationship between ΔU_P and W_M for the conditions given for Figure 7. This illustrates the solution for W_L.

ions with W_M=5.4 keV. In this case there is a closed westward path around the Earth inside of $\mathcal{L}_0$, and there is a separate sunward path open to the tail on the dawn side of the Earth. This path is similar to Lines C and D of Figure 7. The point of measurement is on the path open to the tail. Line B shows the path for ions with W_M=9.4 keV. This energy is labeled W_S to indicate the stagnation energy which is discussed in Section 7. Here the inner closed westward path joins with the outer open path at a single point on the dawn meridian near 3.2 R_E, and the point of measurement is located on the outer open path. Line D shows the path for ions with W_M=10.8 keV. Here the inner westward path is joined with the outer open path to form a single open path that crosses the dawn-dusk meridian on the dusk side of the Earth. Line E shows the path for ions with $W_M = W_H$. This path is similar to Line B except that the point of measurement is now located on the inner closed path. This is the transition trajectory between open and closed drift paths, because all ions with $W_M < W_H$ are on open paths while higher energies, as shown by Lines F and G, place the point of measurement on closed westward paths. In the last two cases, the open paths from the tail are separate from the open sunward paths.

W_H is calculated in a manner similar to W_C except that ΔU is evaluated to find a single solution at dawn instead of dusk. Figure 12 shows ΔU as a function of L-shell at dawn for the conditions given for Figure 11. Algorithm 6 is used to calculate ΔU, and each curve shows ΔU versus L-shell at dawn for the same six values of W_M and for the

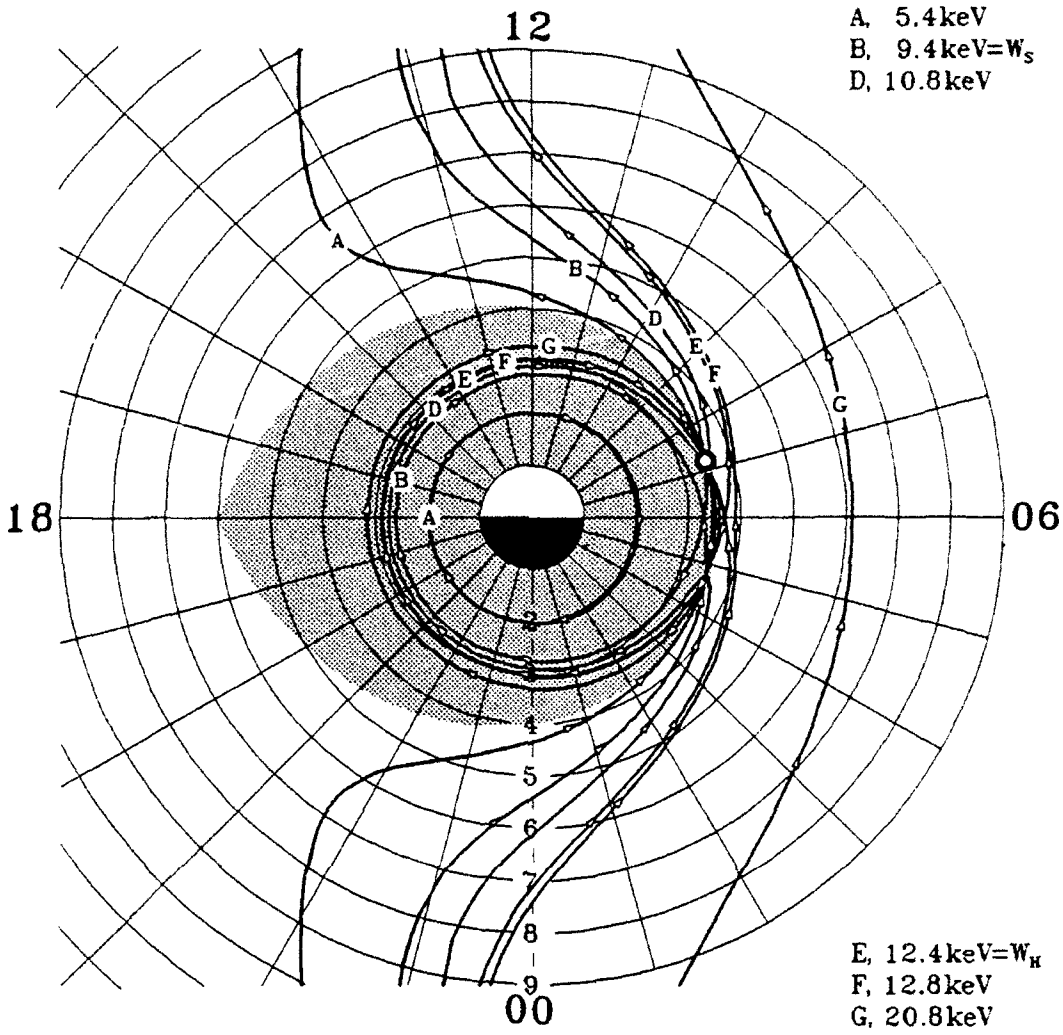

Figure 11 Convection paths of singly charged ions measured at the white circle for six values of W_M. The shaded region is bounded by $\mathcal{L}_0$, and arrows show the direction of drift along the paths.

same measured location given for Figure 11. A seventh energy is included for Curve C. The peaks in this figure look very similar to those seen in Figure 4 for electrons at dusk. Curve E shows the solution for W_H because it gives a single solution of $\Delta U=0$ at dawn while placing the point of measurement on the inner closed path. The peak values of ΔU at dawn are referred to as ΔU_P.

In order to determine the value of ΔU_P, the L-shell L_P at dawn at which the peak occurs is identified, so that $\Delta U_P=\Delta U(L_P)$. L_P occurs at the L-shell where $\partial\Delta U/\partial L=0$ at dawn. $\Delta U=U_M-U$, and U comes from Eq. (5) with $q=1$ and $\sin(\phi)=1$, so that

$$\frac{\partial \Delta U}{\partial L}(L=L_P) = -\frac{\partial W}{\partial L}(L=L_P) - \gamma a A L_P^{\gamma-1} - B_0 a^2 \omega L_P^{-2} = 0 \qquad (25)$$

This solution is identical to Eq. (22) except for the sign change in the second term. It is solved iteratively as is Eq. (11) by using Eq. (15), except that the solution of interest

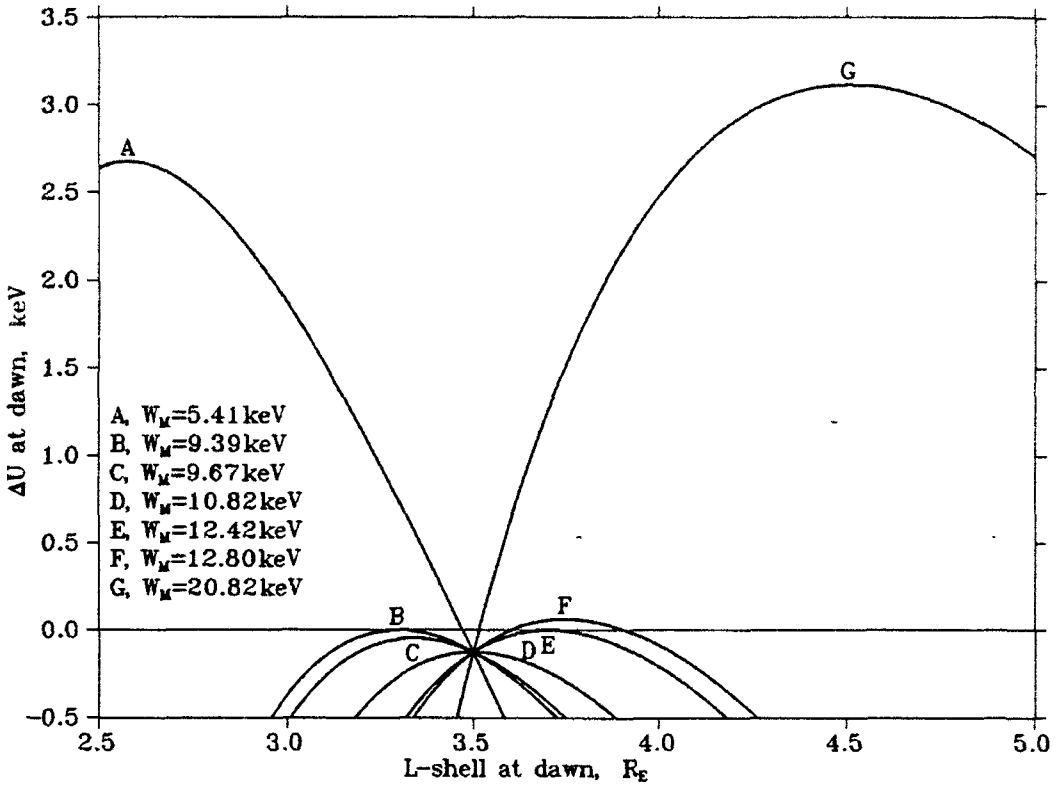

Figure 12 ΔU as a function of L-shell at dawn ($\sin(\phi)=1$) for the same conditions, measured location, and energies as those given for Figure 11.

is that given by Eq. (17) where $Q_A=-\gamma aA$, $Q_B=-B_0a^2\omega-c_1$, and $Q_C=-c_2$. The values of c_1 and c_2 of Eq. (15) are first determined from initial points at $L=L_0$ and $L=L_0$-1. An estimate of L_P is determined using Eq. (17), and this new value is used to replace the initial estimated value of L-shell farthest from the new estimate. New values for c_1 and c_2 are determined, which then give a better estimate of L_P. This process is repeated until it converges to a solution, usually in four to five iterations. Algorithm 12 shows this method of determining L_P.

Figure 13 illustrates Algorithm 12 for the solution of L_P for the case $W_M=W_H$, Curve E of Figure 12. The bold line shows $\partial\Delta U/\partial L$ as a function of L-shell at dawn. L_P is located where this line crosses zero (Point U). Points P and Q at $L=L_0$ and $L=L_0$-1 are used to determine initial values for c_1 and c_2 [Eq. (15)]. Line u, which is a thin solid line, shows the approximation to $\partial\Delta U/\partial L$ by using Eq. (15). Because the approximation is close to the actual solution, Line u', which is a thin dashed line, is shown with the error between the approximation and the actual solution exaggerated by a factor of 50. Equation (17) is used to identify the zero intersect of Line u at Point R. The second iteration uses Points Q and R to give Line v which yields Point S. This method is iterated two more times to yield Points T and U before it stops.

W_H is determined by identifying the value of W_M which gives $\Delta U_P=0$. The initial value used to determine W_H is found in a manner similar to that for W_C given by Eq.

Algorithm 12 Calculation of L_P at dawn for given values of μ and J for ions.

```
FUNCTION DEFINITION OF PeakW_H(μ, J)
local constants required for PeakW_H(μ, J):
        k ≡ -B_0·a^2·ω
local variables required for PeakW_H(μ, J):
        L, L_1, L_2              These hold the current solutions of L-shell
        D, D_1, D_2              These hold ∂W/∂L for the current solutions of L-shell
        c_1, c_2, Q_A, Q_B, Q_Q
implementation of PeakW_H(μ, J):
        L_1 = L_0                Find two starting points for the iteration.
        D_1 = ∂W/∂L(μ, J, L_1)   L_0 is usually within a few R_E of the final solution.
        L_2 = L_1 - 1.0
        D_2 = ∂W/∂L(μ, J, L_2)
        Q_A = -γ·a·A             First coefficient for Equation 17.
        while abs(L_2-L_1) > δ_L repeat the following loop:
                begin while loop
                c_2 = (L_1^2·D_1 - L_2^2·D_2) / (L_1^(-γ-1) - L_2^(-γ-1))   Solution to Equation 15
                c_1 = L_1^2·D_1 - c_2·L_1^(-γ-1)                            coefficients.
                Q_B = k - c_1                    Second coefficient for Equation 17.
                Q_Q = Q_B^2 + 4·Q_A·c_2          Value inside of root in Equation 17.
                L = [½(-Q_B - Q_Q^½)/Q_A]^(1/(γ+1))   Equation 17 yields better value for L.
                D = ∂W/∂L(μ, J, L)               New value for ∂W/∂L is computed.
                if abs(L - L_1) < abs(L - L_2) then   Replace whichever solution is
                        begin conditional block       farthest from new solution.
                        L_2 = L
                        D_2 = D
                        end conditional block
                else
                        begin conditional block
                        L_1 = L
                        D_1 = D
                        end conditional block
                end while loop
        return value of L
```

(21). Because the sign of q is changed and the sign of $\sin(\phi)$ is changed, there are some sign changes in Eq. (21), giving

$$W_0 = -W_{arry}\left(\gamma a A L_M^{\gamma-1} + B_0 \omega a^2 L_M^{-2}\right)\left[\frac{\partial W}{\partial L}(W=W_{arry}, L=L_M)\right]^{-1} \qquad (26)$$

Algorithm 13 shows the implementation of the iterative search used to find W_H for a position given as $y=y_M$, $L=L_M$, and $\sin(\phi)=s_M$. The initial lower value of W_M for the search is given by Eq. (26). This equation always gives a positive solution. The initial upper value is chosen arbitrarily to be 10 keV greater than the lower value. A third point is picked by assuming that the first two points lie on parabola, and that the slope of the parabola is zero at the lower point. A parabola is used to approximate the relationship between ΔU_P and W_M using three points, and it is used to solve for a new value of W_M. The point that is farthest from $\Delta U_P=0$ is replaced by the new solution for W_M for the next iteration. The iteration is continued until the value of $W_H=W_M$ is known to

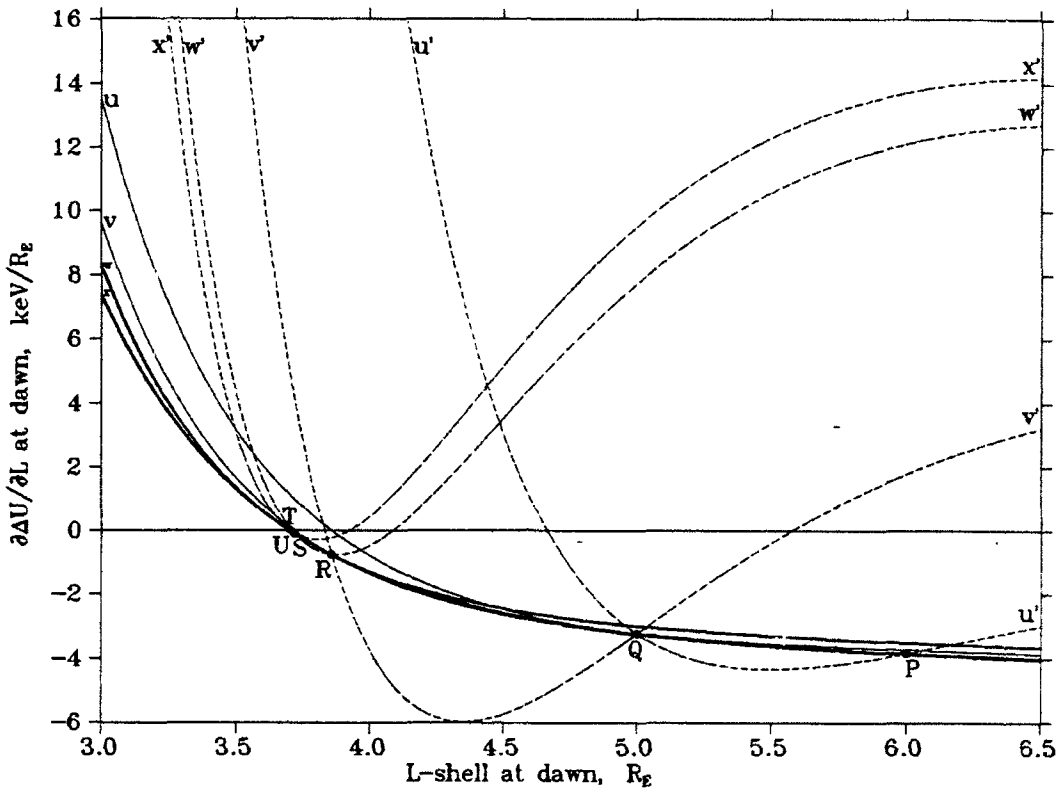

Figure 13 Slope of Curve E in Figure 12. The bold line is the actual slope, and the thin solid lines are approximations using Equation 15. The dashed lines exaggerate the error between the approximations and actual slope by a factor of 50.

sufficient accuracy, usually in about three iterations.

Figure 14 illustrates the solution for W_H for the conditions given for Figure 13. Points A through G have the same energy as those in the previous figure. The x axis shows W_M, the y axis shows ΔU_P, and the dark curve shows the relationship between the two. The initial lower boundary at Point D is identified using Eq. (26), and the initial upper boundary at Point G is found by adding 10 keV to the energy of Point D. Point F is found using the zero intercept of the parabola formed from Points D and G with a slope of zero at Point D (shown by thin dotted line). The zero intercept of the parabola formed from these three points (thin solid line) is very close to the true solution shown by Point E. The process converges to Point E on the next iteration.

7. CALCULATION OF ION STAGNATION ENERGY, W_S

The ion stagnation energy, W_S, is the energy for which ions on open drift paths switch from crossing the dawn-dusk meridian on the dawn side to crossing on the dusk side. This energy is called a stagnation energy because ions with this energy move through a stagnation point on the dawn side of the Earth, even though they may still be on open drift paths. The significance of W_S is discussed in Kerns *et al.* [1993]. Figure

Algorithm 13 Calculation of ion upper cutoff energy, W_H, for a position given by L, y, and $\sin(\phi)$.

FUNCTION DEFINITION OF $W_H(y, L, s)$
local constants required for $W_H(y, L, s)$:
$k \equiv B_0 \cdot \omega \cdot a^2$
local variables required for $W_H(y, L, s)$:
$U_0, \mu_1, J_1, W_0, W_1, W_2, \Delta U_0, \Delta U_1, \Delta U_2, Q_A, Q_B, Q_C$
implementation of $W_H(y, L, s)$:
$\mu_1 = \mu(y, 1, L)$ *Value of μ at y,L,s if W=1 eV; $\mu = \mu_1 \cdot W$ Eqn 3*
$J_1 = J(y, 1, L)$ *Value of J at y,L,s if W=1 eV; $J = J_1 \cdot W^{\gamma}$ Eqn 4*
$U_0 = U(\text{false}, 0, L, s)$ *Value of U at y,L,s if W=0 eV; $U = U_0 + W$ Eqn 5*
$W_0 = -W_{step} \cdot (k/L^2 + \gamma \cdot a \cdot A \cdot L^{\gamma-1}) / \partial W/\partial L(\mu_1 \cdot W_{step}, J_1 \cdot W_{step}^{\gamma}, L)$ *Equation 26*
$\Delta U_0 = \Delta U(\mu_1 \cdot W_0, J_1 \cdot W_0^{\gamma}, U_0 + W_0, \text{false}, \text{PeakW}_H(\mu_1 \cdot W_0, J_1 \cdot W_0^{\gamma}), 1)$ ★
The second starting point is offset from the first by W_{step}.
$W_1 = W_0 + W_{step}$
$\Delta U_1 = \Delta U(\mu_1 \cdot W_1, J_1 \cdot W_1^{\gamma}, U_0 + W_1, \text{false}, \text{PeakW}_H(\mu_1 \cdot W_1, J_1 \cdot W_1^{\gamma}), 1)$ ★
A parabolic approximation is used to find the third point. It uses the points W_0 and W_1, and assumes the slope at W_0 is zero.
$W_2 = W_0 + W_{step} \cdot [\Delta U_0/(\Delta U_0 - \Delta U_1)]^{\gamma}$ *This is zero intercept of parabola.*
$\Delta U_2 = \Delta U(\mu_1 \cdot W_2, J_1 \cdot W_2^{\gamma}, U_0 + W_2, \text{false}, \text{PeakW}_H(\mu_1 \cdot W_2, J_1 \cdot W_2^{\gamma}), 1)$ ★
Reorder W_0, W_1, and W_2 so that $|\Delta U_0| < |\Delta U_1| < |\Delta U_2|$
if $\text{abs}(\Delta U_1) < \text{abs}(\Delta U_0)$ then
swap values of ΔU_1 with ΔU_0 and W_1 with W_0
if $\text{abs}(\Delta U_2) < \text{abs}(\Delta U_1)$ then
swap values of ΔU_2 with ΔU_1 and W_2 with W_1
if $\text{abs}(\Delta U_1) < \text{abs}(\Delta U_0)$ then
swap values of ΔU_1 with ΔU_0 and W_1 with W_0
while $\text{abs}(W_1 - W_0) > \delta_W \cdot (W_0 + W_1)$ repeat following loop:
begin *while loop*
$Q_A = [\Delta U_0 \cdot (W_2 - W_1) + \Delta U_1 \cdot (W_0 - W_2) + \Delta U_2 \cdot (W_1 - W_0)] /$
$[W_0^2 \cdot (W_2 - W_1) + W_1^2 \cdot (W_0 - W_2) + W_2^2 \cdot (W_1 - W_0)]$
$Q_B = [\Delta U_0 - \Delta U_1 - Q_A \cdot (W_0^2 - W_1^2)] / (W_0 - W_1)$
$Q_C = \Delta U_0 - W_0 \cdot (Q_B + Q_A \cdot W_0)$
$\Delta U_2 = \Delta U_1$ *Shift point 1 to point 2*
$W_2 = W_1$ *and point 0 to point 1,*
$\Delta U_1 = \Delta U_0$ *and find new point 0.*
$W_1 = W_0$
$W_0 = \frac{1}{2} \cdot [-Q_B + (Q_B^2 - 4 \cdot Q_A \cdot Q_C)^{\gamma}] / Q_A$ *Quadratic Formula*
$\Delta U_0 = \Delta U(\mu_1 \cdot W_0, J_1 \cdot W_0^{\gamma}, U_0 + W_0, \text{false}, \text{PeakW}_H(\mu_1 \cdot W_0, J_1 \cdot W_0^{\gamma}), 1)$ ★
end *while loop*
return value of W_0

★ *These lines can be made more efficient by calculating $\mu_1 \cdot W_n$ and $J_1 \cdot W_n^{\gamma}$ only once for each line instead of twice.*

---

11 illustrates the ion stagnation energy, W_S. In this figure Lines A, B, and D place the point of measurement on an open drift path. Line A, which has $W_M < W_S$ crosses the dawn-dusk meridian on the dawn side of the Earth. Line D, which has $W_M > W_S$ crosses the dawn-dusk meridian on the dusk side of the Earth. Line B shows $W_M = W_S$, and here the closed inner path meets the open outer path at a single point at dawn. Although the point of measurement is on an open field line, ions convecting from the tail move through the dawn stagnation point to reach the point of measurement, and cannot convect to the point of measurement.

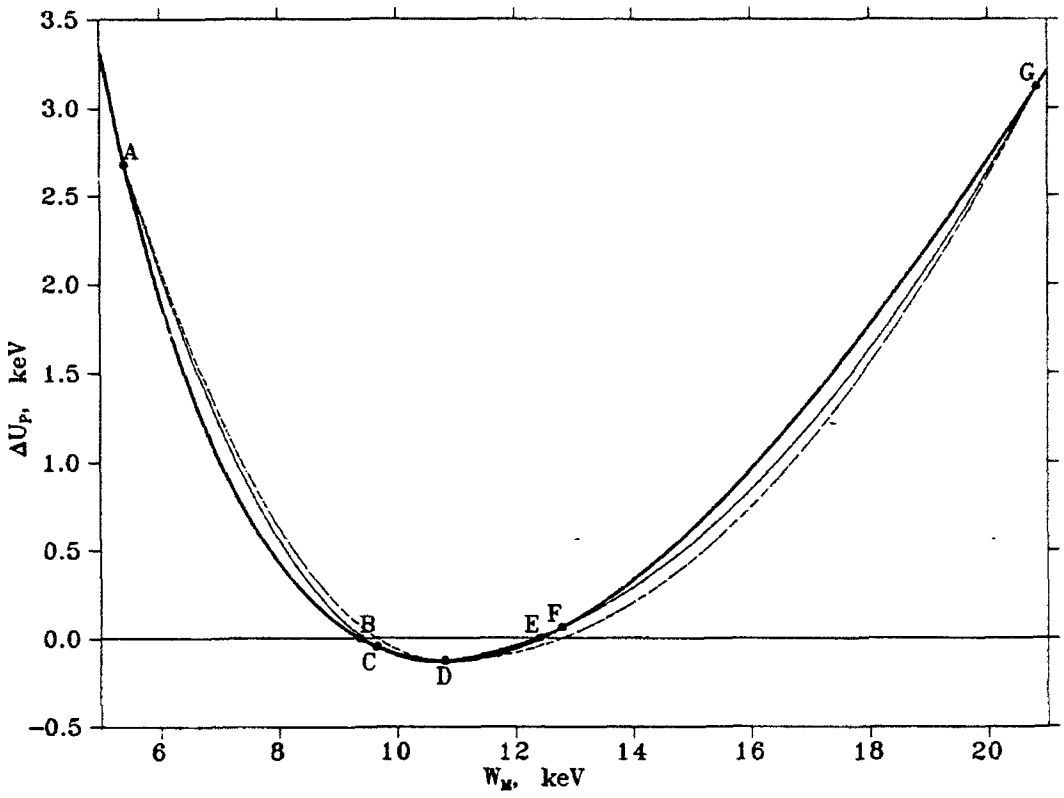

Figure 14 Relationship between ΔU_P and W_M for the conditions given for Figure 13. This illustrates the solutions for W_H and W_S.

W_S is calculated in a manner identical to that of W_H except that Eq. (26) gives the initial upper value instead of the initial lower value of W_M in the search. Also, the quadratic formula uses the negative solution to find the zero intercept of the approximating parabolas. The upper solution to $\Delta U_P=0$ is shown by Curve E in Figure 12 where $W_M=W_H$. The lower solution to $\Delta U_P=0$ is shown by Curve B, and here $W_M=W_S$. Curve D uses the value given by Eq. (26) for W_M, and as can be seen in the figure, W_S is less than this value. The location of the peaks are determined using Algorithm 12.

Algorithm 14 shows the implementation of the iterative search used to find W_S for a position given as $y=y_M$, $L=L_M$, and $\sin(\phi)=s_M$. The initial upper value of W_M for the search is given by Eq. (26). This equation always gives a positive solution. The initial lower value is set to one-half the initial upper value. A third point is picked by assuming the first two points lie on parabola, and the slope of the parabola is zero at the upper point. If W_M for the third point is less than or equal to zero, then W_M for this point is set to one-half the lower value. A parabola is used to approximate the relationship between ΔU_P and W_M using three points, and it is used to solve for a new value of W_M. The point which is farthest from $\Delta U_P=0$ is replaced by the new solution for W_M for the next iteration. The iteration is continued until the value of $W_S=W_M$ is known to sufficient accuracy, usually in about three iterations.

Algorithm 14 *Calculation of ion stagnation energy, W_S, for a position given by L, y, and $\sin(\phi)$.*

FUNCTION DEFINITION OF $W_s(y, L, s)$
local constants required for $W_s(y, L, s)$:
$k \equiv B_0 \cdot \omega \cdot a^2$
local variables required for $W_s(y, L, s)$:
$U_0, \mu_1, J_1, W_0, W_1, W_2, \Delta U_0, \Delta U_1, \Delta U_2, Q_A, Q_B, Q_C$
implementation of $W_s(y, L, s)$:
$\mu_1 = \mu(y, 1, L)$ *Value of μ at y,L,s if W=1 eV; $\mu = \mu_1 \cdot W$* *Eqn 3*
$J_1 = J(y, 1, L)$ *Value of J at y,L,s if W=1 eV; $J = J_1 \cdot W^{½}$* *Eqn 4*
$U_0 = U(\text{false}, 0, L, s)$ *Value of U at y,L,s if W=0 eV; $U = U_0 + W$* *Eqn 5*
$W_0 = -W_{step} \cdot (k/L^2 + \gamma \cdot a \cdot A \cdot L^{r-1}) / \partial W/\partial L(\mu_1 \cdot W_{step}, J_1 \cdot W_{step}^{½}, L)$ *Equation 26*
$\Delta U_0 = \mathbf{\Delta U}(\mu_1 \cdot W_0, J_1 \cdot W_0^{½}, U_0 + W_0, \text{false}, \mathbf{PeakW_H}(\mu_1 \cdot W_0, J_1 \cdot W_0^{½}), 1)$ ★
The second starting point is offset from the first by W_{step}.
$W_1 = ½W_0$
$\Delta U_1 = \mathbf{\Delta U}(\mu_1 \cdot W_1, J_1 \cdot W_1^{½}, U_0 + W_1, \text{false}, \mathbf{PeakW_H}(\mu_1 \cdot W_1, J_1 \cdot W_1^{½}), 1)$ ★
A parabolic approximation is used to find the third point. It uses the points W_0 and W_1, and assumes the slope at W_0 is zero.
$W_2 = W_0 - (W_0 - W_1) \cdot [\Delta U_0 / (\Delta U_0 - \Delta U_1)]^{½}$ *This is zero intercept of parabola.*
if $W_2 \le 0$ **then**
$W_2 = ½W_1$
$\Delta U_2 = \mathbf{\Delta U}(\mu_1 \cdot W_2, J_1 \cdot W_2^{½}, U_0 + W_2, \text{false}, \mathbf{PeakW_H}(\mu_1 \cdot W_2, J_1 \cdot W_2^{½}), 1)$ ★
Reorder W_0, W_1, and W_2 so that $|\Delta U_0| < |\Delta U_1| < |\Delta U_2|$
if $\text{abs}(\Delta U_1) < \text{abs}(\Delta U_0)$ **then**
swap values of ΔU_1 with ΔU_0 and W_1 with W_0
if $\text{abs}(\Delta U_2) < \text{abs}(\Delta U_1)$ **then**
swap values of ΔU_2 with ΔU_1 and W_2 with W_1
if $\text{abs}(\Delta U_1) < \text{abs}(\Delta U_0)$ **then**
swap values of ΔU_1 with ΔU_0 and W_1 with W_0
while $\text{abs}(W_1 - W_0) > \delta_W \cdot (W_0 + W_1)$ **repeat following loop:**
begin *while loop*
$Q_A = [\Delta U_0 \cdot (W_2 - W_1) + \Delta U_1 \cdot (W_0 - W_2) + \Delta U_2 \cdot (W_1 - W_0)] /$
$[W_0^2 \cdot (W_2 - W_1) + W_1^2 \cdot (W_0 - W_2) + W_2^2 \cdot (W_1 - W_0)]$
$Q_B = [\Delta U_0 - \Delta U_1 - Q_A \cdot (W_0^2 - W_1^2)] / (W_0 - W_1)$
$Q_C = \Delta U_0 - W_0 \cdot (Q_B + Q_A \cdot W_0)$
$\Delta U_2 = \Delta U_1$ *Shift point 1 to point 2*
$W_2 = W_1$ *and point 0 to point 1,*
$\Delta U_1 = \Delta U_0$ *and find new point 0.*
$W_1 = W_0$
$W_0 = ½ \cdot [-Q_B - (Q_B^2 - 4 \cdot Q_A \cdot Q_C)^{½}] / Q_A$ *Quadratic Formula*
if $W_0 \le 0$ **then**
$W_0 = ½W_1$
$\Delta U_0 = \mathbf{\Delta U}(\mu_1 \cdot W_0, J_1 \cdot W_0^{½}, U_0 + W_0, \text{false}, \mathbf{PeakW_H}(\mu_1 \cdot W_0, J_1 \cdot W_0^{½}), 1)$ ★
end *while loop*
return value of W_0
★ *These lines can be made more efficient by calculating $\mu_1 \cdot W_n$ and $J_1 \cdot W_n^{½}$ only once for each line instead of twice.*

Figure 14 illustrates the solution for W_S for the conditions given for Figure 13. The initial upper boundary at Point D is identified using Eq. (26), and the initial lower boundary at Point A is one-half the energy of Point D. Point C is found using the zero intercept of the parabola formed from Points D and A with a slope of zero at Point D

(shown by thin dotted line). The zero intercept of the parabola formed from these three points (thin solid line) is very close to the true solution shown by Point B. The process converges to Point B on the next iteration.

References

Chen, F.F. (1984), *Introduction to Plasma Physics and Controlled Fusion*, 2nd ed., pp. 19-32, Plenum Press, New York.

Ejiri, M. (1978), Trajectory of charged particles in the magnetosphere, *J. Geophys. Res.*, **83**:4798.

Kerns, K.J., Hardy, D.A., and Gussenhoven M.S. (1993), Modelling of Convection Boundaries Seen by CRRES in 120 eV to 28 keV Particles, to be published in *J. Geophys. Res.*.

McIlwain, C.E. (1961), Coordinates for mapping the distribution of magnetically trapped particles, *J. Geophys. Res.*, **66**:3681.

Southwood, D.J., and Kaye, S.M. (1979), Drift boundary approximations in simple magnetospheric convection models, *J. Geophys. Res.*, **84**:5773.

Stern, D.P. (1975), The motion of a proton in the equatorial magnetosphere, *J. Geophys. Res.*, **80**:595.

Volland, H. (1973), A semiempirical model of large-scale magnetospheric electric fields, *J. Geophys. Res.*, **78**:171.